Analyses were performed using a FACSCalibur flow cytometer (BD Biosciences) and FlowJo Version 7.2.4 software (TreeStar). The detailed description of these analyses can be found in Supplementary Methods.

Statistical analysis

Frequencies of genomic alterations were evaluated using Fisher exact test, and cumulative acute transformation rates were analyzed using Kaplan–Meier method.

All statistical analyses were performed with EZR (Saitama Medical Center, Jichi Medical University, Saitama, Japan), which is a graphical user interface for R (The R Foundation for Statistical Computing; ref. 21).

Results

Genomic alteration profiles of chronic- and acute-type ATL

To evaluate the genomic alterations of chronic- and acute-type ATL, aCGH was performed for 62 patient samples (27 cases of chronic-type and 35 cases of acute-type ATL; Table 1 and Supplementary Table S1). Figure 1A shows genomic alteration profiles of chronic- and acute-type ATL. We identified 362 MCRs (230 losses and 132 gains) among the alterations. These MCRs contained 1–3 protein-coding genes, which are most likely the candidate genes of the alterations (15, 17). Frequent alterations are supposed to especially contribute to the pathophysiology of the disease. MCRs that were found in

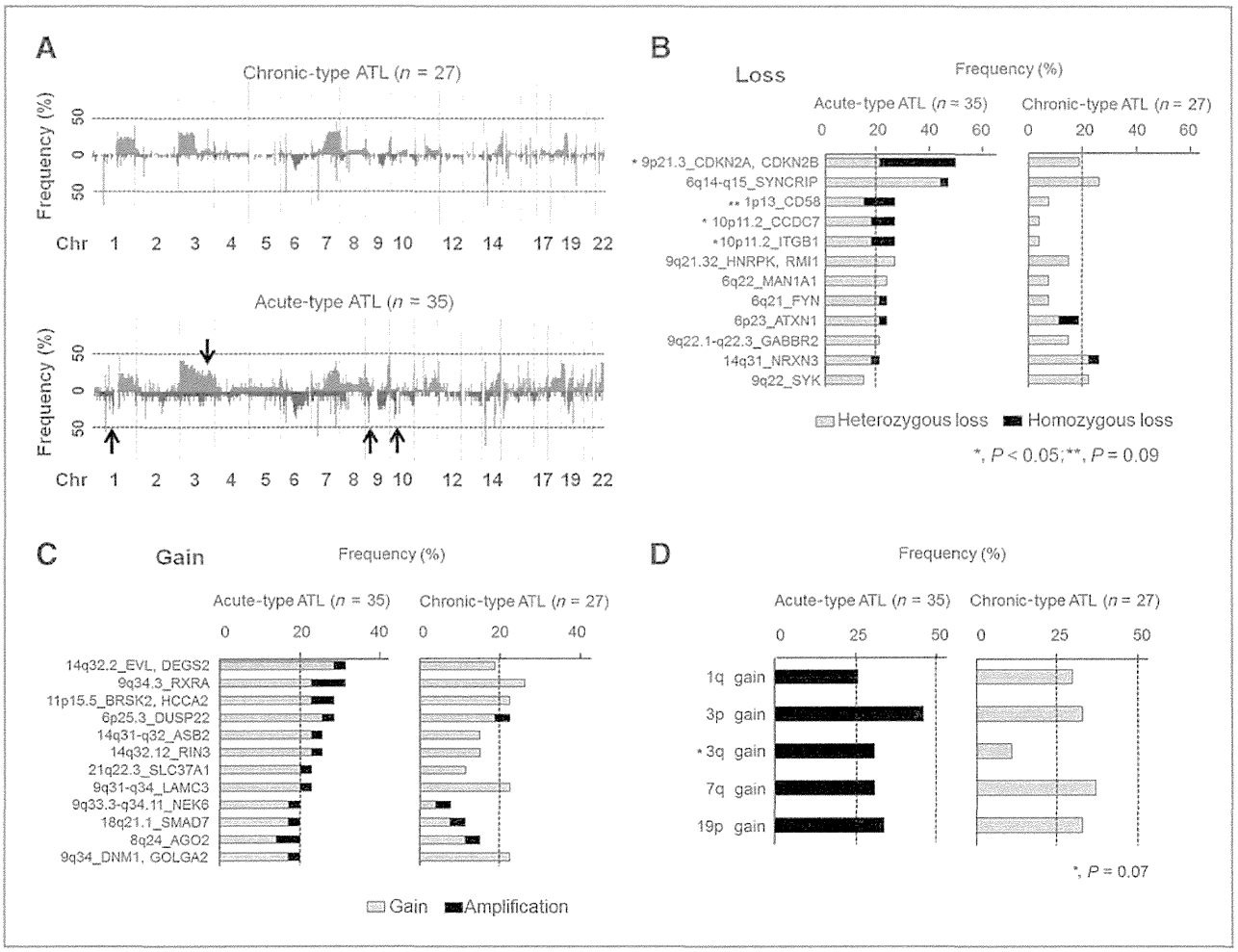

Figure 1. Genomic alteration profiles of chronic- and acute-type ATL. A, frequency of genomic alterations in chronic-type and acute-type ATL. Top, 27 cases with chronic-type ATL; bottom, 35 cases with acute-type ATL. The horizontal axis indicates each probe aligned from chromosome 1 to 22 and the short arm (p) to long arm (q). The vertical axis indicates the frequency of genomic alterations among the analyzed cases. The top area represents gain and the bottom area represents loss. Arrows represent characteristic alterations of acute-type ATL compared with chronic-type. B, MCRs encompassing 1–3 coding genes of copy number loss. MCRs found in greater than 20% of chronic-type or acute-type ATL are shown and ranked by frequency of alteration (left, acute type; right, chronic type). Among these MCRs, loss of *CDKN2A/CDKN2B* located in 9p21.3, losses of *CCDC7* and *ITGB1* located in 10p11.2 were observed more frequently in acute-type ATL. Loss of *CD58* was also found more frequently in acute type than in the chronic type (Fisher exact test; *, $P < 0.05$; **, $P = 0.09$). Frequently altered MCRs in chronic-type ATL were also recognized in the acute type. C, MCRs of copy number gain. MCRs found in greater than 20% of chronic-type or acute-type ATL are shown and ranked by frequency of alteration (left, acute type; right, chronic type). None of these MCRs were characteristic of acute-type or chronic-type ATL. D, gains of chromosomes 1q, 3p, 3q, 7q, and 19p were observed in greater than 20% of acute-type and chronic-type ATL. MCRs were not detected in any of these lesions. Gain of 3q was more frequently found in acute-type ATL than in the chronic type (*, $P = 0.07$).

more than 20% of chronic- or acute-type ATL were therefore analyzed (Fig. 1B and C).

Genomic loss of *CDKN2A/CDKN2B* was the first most frequently altered MCR in acute-type ATL (17 of 35 cases). The second most frequently altered MCR of acute-type ATL was genomic loss of *SYNCRIP* (16 of 35 cases). On the other hand, genomic losses of *SYNCRIP* and *NRXN3* and gain of *RXRA* were most frequently altered MCRs in chronic-type ATL (7 of 27 cases). Among these identified MCRs, the losses of *CDKN2A/CDKN2B*, *CCDC7*, and *ITGB1* were significantly characteristic of acute-type ATL (Fig. 1B, $P < 0.05$). In addition, acute-type ATL tended to have a loss of *CD58* (Fig. 1B). The frequently altered MCRs in chronic-type ATL were also found in acute-type ATL (Fig. 1B and C). Gains of chromosomes 1q, 3p, 3q, 7q, and 19p were also frequently observed in acute- and chronic-type ATL, although they did not show MCRs (Fig. 1D). Among these alterations, acute-type ATL tended to have a gain of 3q ($P = 0.07$).

Frequent loss of CDKN2A/CDKN2B

Our analysis identified loss of *CDKN2A/CDKN2B* located in 9p21.3 as the most frequently and specifically altered genomic region in acute-type ATL compared with chronic-type ATL. Therefore, this loss is suggested to play an important role in the pathophysiology of acute-type ATL and acute transformation of chronic-type ATL.

Seventeen of the 35 acute-type ATL samples showed loss of 9p21.3, which was also found in 5 of the 27 chronic-type ATL samples. These losses always included *CDKN2A/CDKN2B* (Fig. 2A). Homozygous loss of *CDKN2A/CDKN2B* was observed in 10 of the 17 affected acute-type ATL samples but was never observed in chronic-type ATL. The genes whose expression was affected by copy number changes are considered candidate genes in the regions of genomic alterations (15, 22, 23). We therefore evaluated the expressions of CDKN2A and CDKN2B in acute-type and chronic-type ATL with or without loss of 9p (Fig. 2B). CDKN2A expression was much lower in acute-type ATL samples with the loss of 9p than in other samples. CDKN2B expression was not reduced in accordance with the loss of 9p. Therefore, CDKN2A is a likely candidate tumor suppressor gene located in 9p21.3.

Serial samples of a patient with chronic-type ATL showing acute transformation were analyzed in detail. The DNA and RNA samples of this patient at about 19 months before acute transformation (chronic phase, C-10) and at acute transformation (acute phase, A-15) were available. Clonality analysis of T-cell receptor gamma locus showed that clones of ATL cells at chronic and acute phases were identical to each other (Supplementary Fig. S1B). Although the chronic-phase sample showed heterozygous loss of *CDKN2A/CDKN2B*, the acute-phase sample showed homozygous loss of *CDKN2A/CDKN2B* (Fig. 2C). In addition, the expression of CDKN2A was remarkably reduced in the acute phase (Fig. 2D). Analysis of these serial samples of an identical patient also indicated that CDKN2A is the most likely candidate gene located in 9p21.3 and that the loss of *CDKN2A* is associated with acute transformation.

Frequently altered cell-cycle pathway in acute-type ATL

CDKN2A contains 2 known transcriptional variants, *INK4a* (*p16*) and *ARF* (*p14*). Both of these genes are known to be negative regulators of the cell cycle. We next evaluated the distributions of genomic alterations of *CDKN2A* with other genes that were previously reported to affect the cell cycle (Fig. 2E; ref. 24). Our analysis revealed that losses of *CDKN2A* and losses of *TP53* tended to be mutually exclusive events, and this pattern was also observed for losses of *TP53* and gains of *MDM4/RFWD2*. These alterations of cell-cycle–related genes were specifically observed in acute-type ATL compared with chronic-type ATL (80% of acute-type and 56% of chronic-type ATL, $P < 0.05$; Fig. 2F). Among chronic-type ATL cases, those with acute transformation tended to have alterations of cell-cycle–related genes (Fig. 2G). GSEA also revealed that the cell-cycle–related gene set and genes functionally associated with proliferation were significantly enriched in acute-type ATL compared with chronic-type ATL (Supplementary Fig. S1C).

These results indicated that alterations of the cell-cycle pathway, including the genomic loss of *CDKN2A*, played critical roles in the pathophysiology of acute-type ATL and acute transformation of chronic-type ATL. *In vitro* assays showed that inductions of INK4a or ARF that are encoded by *CDKN2A* caused suppression of cell proliferation, cell-cycle arrest, and apoptosis in ATL cell lines with genomic loss of 9p21.3 (Supplementary Fig. S2).

Genomic alterations of CD58 in ATL

In addition to loss of *CDKN2A/CDKN2B*, we found that losses of *CCDC7*, *ITGB1*, and *CD58* and gain of chromosome 3q were more frequently recognized in acute-type ATL than in chronic-type ATL. Alterations of cell-cycle–related genes, including *CDKN2A*, are considered important events for the transformation described above. We therefore analyzed the distributions of alterations of cell-cycle–related genes and the genes that were characteristic of acute-type ATL in each type of ATL case (Fig. 3). This analysis revealed that alterations of cell-cycle–related genes and the gene alterations characteristic of acute-type ATL mainly coexisted. A case having the loss of *CD58* or gain of 3q without alterations of cell cycle existed for each type of ATL, although all cases with losses of *ITGB1* and *CCDC7* showed the alterations of cell-cycle–related genes.

In chronic-type ATL cases without alterations of cell-cycle–related genes, a case with loss of *CD58* showed acute transformation later, although a case with gain of 3q did not exhibit the transformation without any therapy during 30 months after the diagnosis. *CD58* is a gene known to be involved in activation of natural killer (NK) cells and cytotoxic T cells (CTL; refs. 25, 26). Inactivation of *CD58* is reported to play an important role in the pathophysiology of diffuse large B-cell lymphoma (DLBCL) through the mechanism of escape from the immunosurveillance system (20). Recurrent mutation of *CD58* has also been observed recently in PTCLs (19). We therefore further analyzed *CD58* in ATL.

Analyses using aCGH revealed that 26% (9 of 35) of acute-type ATL and 7% (2 of 27) of chronic-type ATL had genomic loss of 1p13 (Figs. 1B and 4A). These losses always included *CD58* and one case showed genomic loss that only included

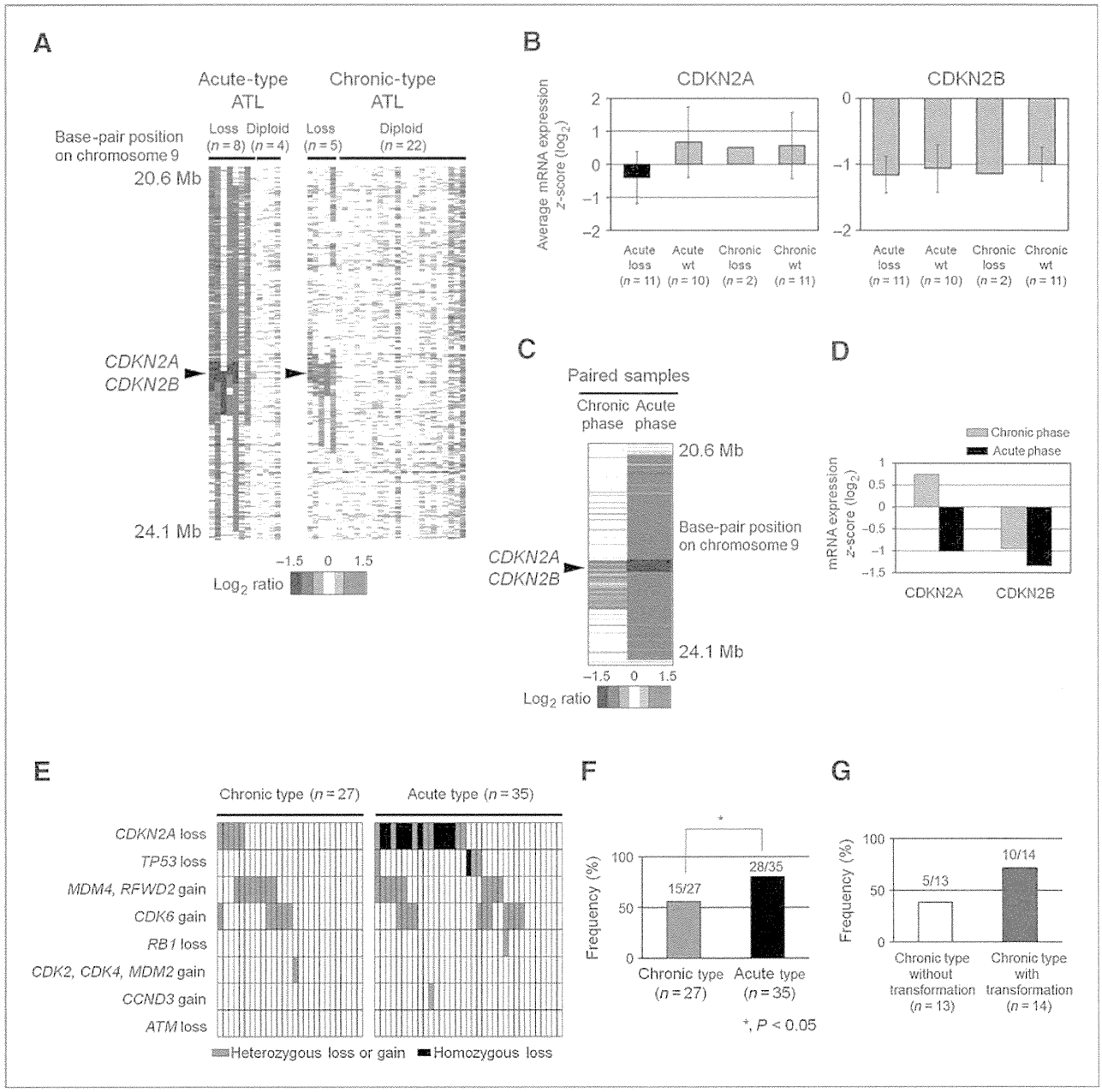

Figure 2. Loss of 9p was mainly observed in acute-type ATL and not chronic-type ATL. A, genomic alterations of chromosome 9p, including *CDKN2A/CDKN2B*. Heatmap analysis of 400K aCGH shows $\log_2$ ratios of tumor cells relative to normal controls. White, blue, and red represent diploid, loss, and gain, respectively. Arrowhead, the *CDKN2A/CDKN2B* locus. B, gene expression levels of CDKN2A and CDKN2B. Gene expression levels of CDKN2A and CDKN2B were analyzed in 13 chronic-type and 21 acute-type ATL cases by GEP. Average gene expressions and SDs are shown in cases grouped as indicated. CDKN2A expression was reduced only in acute-type ATL cases exhibiting loss of *CDKN2A/CDKN2B*. CDKN2B expression did not change in relation to genomic loss or subtype. Probes of A_23_P43484 (CDKN2A) and A_23_P216812 (CDKN2B) were used in experiments. C, genomic alteration of 9p in serial samples of a case with chronic type showing acute transformation. Left, a heatmap of the $\log_2$ ratio in the chronic phase; right, a heatmap of the ratio in the acute phase. The sample in the chronic phase indicates a heterozygous loss of the *CDKN2A/CDKN2B* locus and the loss changes to a homozygous loss for the sample in the acute phase. D, gene expressions of CDKN2A and CDKN2B in serial samples. CDKN2A expression was remarkably reduced in the acute phase, but CDKN2B expression was almost identical during transformation in this case. Gray, the chronic phase; black, the acute phase. E, alterations of cell-cycle–related genes in chronic-type and acute-type ATL. In the heatmap, rows correspond to the indicated alterations and columns represent individual ATL cases. Gray, a heterozygous loss or gain; black, a homozygous loss. Losses of *CDKN2A* and *TP53* tended to be mutually exclusive, and losses of *TP53* and gains of *MDM4/RFWD2* showed a similar tendency. F, alteration frequency of cell-cycle–related genes. Genetic alteration frequency of cell-cycle–related genes was significantly higher in acute-type ATL cases (80%) than in chronic-type ATL (56%; Fisher exact test; *, $P < 0.05$). The actual number of affected samples over the total number analyzed is shown at top of the figure. G, alteration frequency of cell-cycle–related genes among chronic-type ATL cases. The frequency of alterations of cell-cycle–related genes was higher in cases with later acute transformation than in cases without acute transformation.

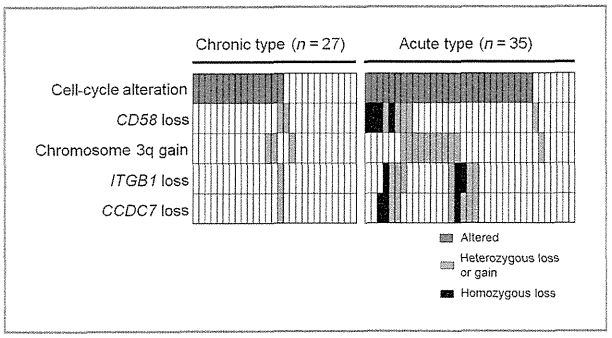

Figure 3. Distribution of genomic alterations frequently observed in acute-type ATL among ATL samples. Heatmap with rows corresponding to the indicated alterations and columns representing individual ATL cases. Gray, a heterozygous loss or gain; black, a homozygous loss. Dark gray also shows the alterations of any cell-cycle–related gene. Alterations frequently found in acute-type ATL were not mutually exclusive of the alteration of cell-cycle–related genes. Cases with losses of *ITGB1* and *CCDC7* always exhibited the alterations of cell-cycle–related genes. Most cases with loss of *CD58* or gain of 3q also exhibited the alterations of cell-cycle–related genes, but a case showing the loss of *CD58* or gain of 3q without disruption of the cell cycle existed in each type of ATL. The loss of *CD58* and gain of 3q were almost mutually exclusive, except for two cases of acute-type ATL.

CD58. Homozygous loss of *CD58* was observed only in acute-type ATL samples. Furthermore, expression of CD58 was reduced in acute-type ATL cases accompanied with the genomic loss (Fig. 4B). Flow cytometric analyses also suggested that genomic loss of *CD58* reduced the expression on the cell surfaces (Fig. 4C). Sequence analysis of *CD58* revealed a nonsense mutation in one acute-type ATL case. This mutation indicated that the 97th position of serine changed to a stop codon (p.S97X; c.290C>A; Fig. 4D). The nontumor cells of this patient showed no mutation, and we therefore regarded this mutation as a somatic mutation. One-nucleotide substitution registered as an SNP in the NCBI database (http://www.ncbi.nlm.nih.gov/gene/) was found in 7 cases (c.43A>G; rs17426456; Supplementary Table S2). Combined with the results of the genomic and mutation analyses, 29% of acute-type and 7% of chronic-type ATL had genetic alteration of *CD58*. These alterations were significantly specific to acute-type ATL compared with chronic-type ATL (Fig. 4E, $P = 0.05$).

In addition to the alteration of *CD58*, inactivation of *B2M* is also reported to play a pivotal role in the immune escape mechanism of DLBCLs (20). Among analyzed cases, only a chronic-type ATL case (C-2) had heterozygous loss of *B2M*, and this case also showed heterozygous loss of *CD58* (Supplementary Table S2). No somatic mutations of *B2M* were observed in ATL cases analyzed.

Genomic alterations predicting acute transformation of chronic-type ATL

We investigated the associations of MCRs that were characteristic of acute-type ATL and that were commonly found in more than 20% of chronic- and acute-type ATL with cumulative acute transformation rates among chronic-type ATL cases (Supplementary Table S3).

Cases exhibiting gain of *RXRA* and loss of *ITGB1*, *CCDC7*, or *CD58* were significantly associated with early progression to acute-type ATL ($P = 0.01$, 0.02, 0.02, and 0.04, respectively; Fig. 5A). Chronic-type ATL cases having the alterations of cell-cycle–related genes also tended to show early progressions to acute-type ATL ($P = 0.07$; Fig. 5B), although cases having only the loss of *CDKN2A* were not significantly associated with the progression (Supplementary Table S3). A chronic-type ATL case with losses of *ITGB1* and *CCDC7* had the alterations of cell-cycle–related genes, and we therefore analyzed the chronic-type ATL cases by the presence of alterations of *CD58* and/or cell-cycle–related genes. This analysis revealed that cases with these alterations were specifically associated with earlier progression to acute-type ATL ($P = 0.03$, Fig. 5C).

Discussion

We have studied 27 cases of chronic-type ATL and compared with 35 cases of acute-type ATL. Until now, only a few chronic-type ATL cases had been analyzed, and the molecular mechanisms of the transformation were investigated by focusing on the well-known tumor suppressor genes (*CDKN2A* and *TP53*; refs. 6–12). In contrast, our investigation comprehensively analyzed genomic profiles, and molecular aspects were analyzed using unbiased and whole-genome methods. Our study of chronic-type ATL represents the largest study to date that has analyzed the whole-genomic status of chronic-type ATL cases. We could identify characteristic molecular profile of chronic-type ATL and could demonstrate possible molecular mechanisms of acute transformation. This study suggested that alterations of cell-cycle–related genes and *CD58* are new predictive implications for chronic-type ATL (Fig. 5C).

Common genomic alterations in chronic- and acute-type ATL

Genomic alteration profiles of chronic- and acute-type ATL were found to be almost identical (Fig. 1). The number of genomic alterations was found to be higher in acute-type ATL than in the chronic-type, and the frequently altered regions of chronic-type ATL were also observed in the acute-type. Thus, chronic-type ATL might be a pre-acute form of the disease.

The common MCRs in chronic- and acute-type ATL included genes involving T-cell receptor signaling, such as *FYN* and *SYK* (27, 28). We also identified *SYNCRIP* as a common MCR in both types of ATL. *SYNCRIP* is a gene known to be involved in maturation of mRNA (29). *RXRA*, which has been reported to be implicated in colorectal carcinogenesis (30), is also frequently altered in both types of ATL. In addition, our analysis suggested that gain of *RXRA* is involved in acute transformation of chronic-type ATL because the chronic-type ATL possessing the gain of *RXRA* showed earlier progression to the acute-type. These MCRs may play important roles in the development of ATL coordinately with HTLV-1.

Deregulation of the cell-cycle pathway: an alteration related to acute transformation

Our analyses of genomic alterations revealed that no single genomic alteration seems to be responsible for the mechanism

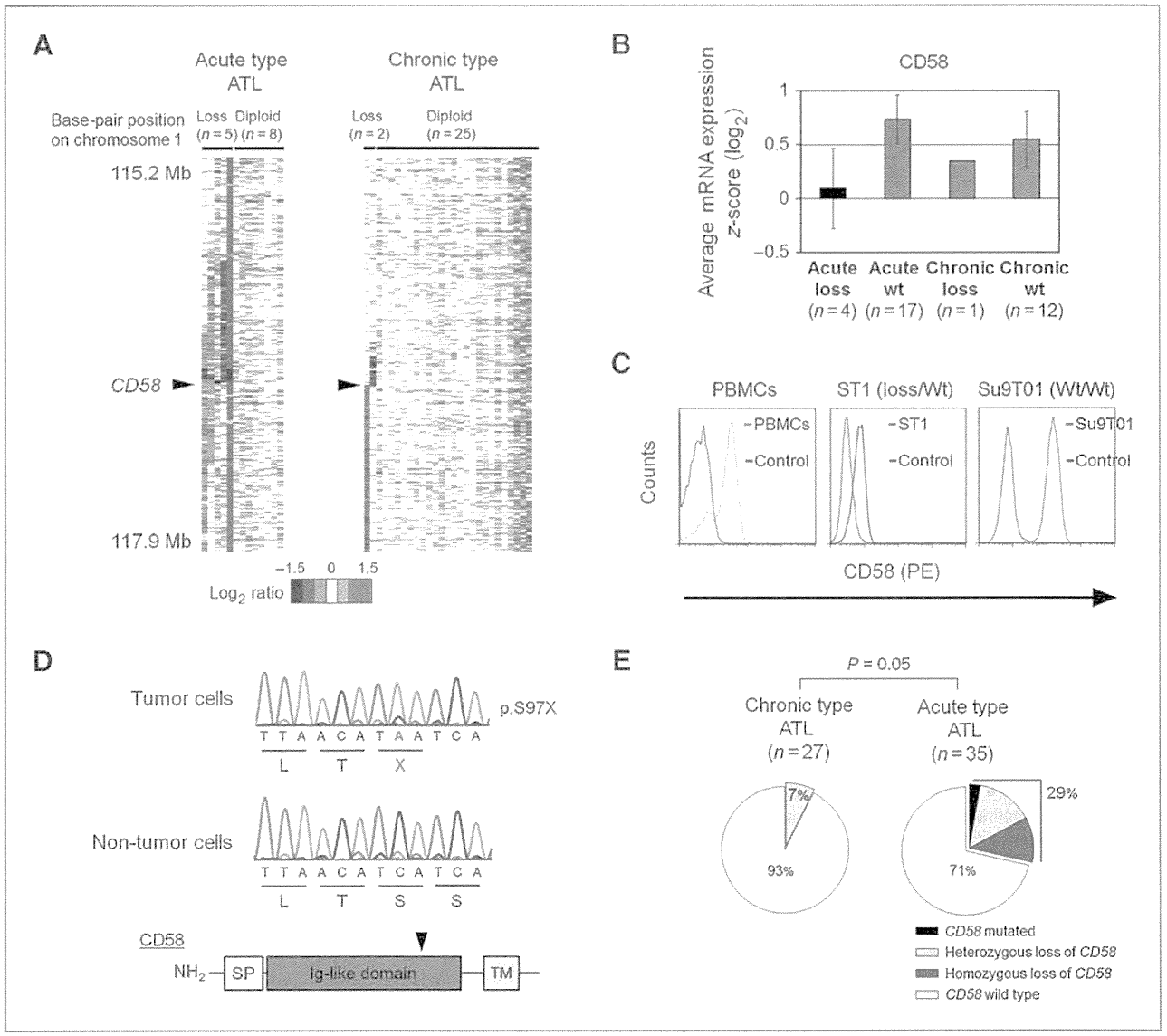

Figure 4. Alteration of *CD58* in acute transformation of chronic-type ATL. A, genomic alterations of chromosome 1p, including *CD58*. Heatmap analysis of 400K aCGH shows $\log_2$ ratios of ATL cases. White, blue, and red represent diploid, loss, and gain, respectively. Arrowhead, the *CD58* locus. B, gene expression levels of CD58. Expression was analyzed in 13 chronic-type and 21 acute-type ATL cases by GEP. Average gene expressions and SDs are shown in cases grouped as indicated. CD58 expression was reduced only in acute-type ATL cases exhibiting loss of *CD58*. Probe A_23_P138308 (CD58) was used in experiments. C, CD58 expressions on ATL cell lines and peripheral blood mononuclear cells (PBMC). Flow cytometric analysis of PBMCs from a healthy donor and two ATL cell lines for surface CD58 expression (orange line, PBMCs; blue line, ST1; red line, Su9T01). ST1 with heterozygous loss of CD58 had the low expression. The gray lines represent the cell lines with the isotype control antibody. D, DNA sequencing chromatogram of an acute-type ATL case (A-35) showing nonsense mutation in exon 2 of *CD58* (top). DNA extracted from nontumor cells (CD4-negative cells in peripheral blood of this patient) did not show the mutation (middle). Bottom, a schematic representation of the CD58 protein depicting the location of the single peptide (SP), Ig-like domain, and transmembrane domain (TM). The inverted triangle indicates the position of the mutation. E, characterization of *CD58* alteration in ATL. Seven percent of chronic-type ATL cases showed genomic loss of *CD58*, whereas 29% of acute-type ATL cases showed genomic alteration of *CD58*, with one case exhibiting mutation (Fisher exact test; $P = 0.05$).

of acute transformation, and various genomic alterations and combinations of alterations exist in this mechanism (Fig. 3). We found that deregulation of the cell cycle, including genomic loss of *CDKN2A*, might be an important event in the transformation. Genomic loss of *CDKN2A* was also reported to play a crucial role in the transformation of chronic lymphocytic leukemia known as Richter syndrome (31, 32).

Although previous studies using Southern blot analysis revealed that 11% to 17% of acute-type ATL had the homozygous loss of *CDKN2A* (7, 9), our analyses using unbiased and whole-genome methods were able to reveal the frequency of the loss in greater detail. We found that approximately 30% of acute-type ATL cases showed a homozygous loss of the *CDKN2A/CDKN2B* locus, and 50% of acute-type ATL cases

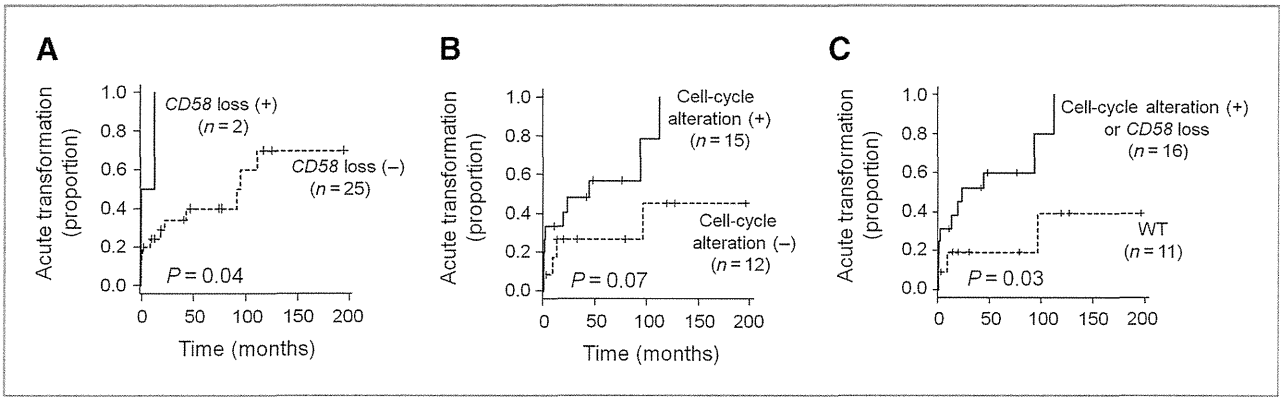

Figure 5. Genomic alterations associated with acute transformation in chronic-type ATL. A, genomic loss of *CD58* was significantly associated with earlier acute transformation ($P = 0.04$). B, chronic-type ATL cases with alterations of cell-cycle–related genes tended to exhibit earlier progression to acute-type ATL ($P = 0.07$). C, cases with either *CD58* loss or alterations of cell-cycle–related genes showed a much shorter time to acute transformation within chronic-type ATL cases ($P = 0.03$).

exhibited the homozygous or heterozygous loss of this locus. Yamagishi and colleagues used high-resolution aCGH analyses and found that this loss was frequently found in ATL samples (33). We also found that 5 of 27 chronic-type ATL cases had heterozygous loss of *CDKN2A*. Three of the 5 cases with *CDKN2A* loss progressed to the acute type, but 11 of the 22 cases without *CDKN2A* loss also showed acute transformation. Because of this finding, *CDKN2A* loss was not significantly associated with the earlier acute transformation in our study (Supplementary Table S3). Although previous studies revealed that approximately 5% of chronic-type had this loss (7, 9, 10), these previous studies did not show the cumulative acute transformation rate according to *CDKN2A* loss.

CDKN2A expression was reduced in acute-type ATL samples exhibiting genomic loss of the *CDKN2A* locus. A portion of acute-type ATL cases without the genomic loss showed a low expression level of CDKN2A, suggesting that methylation of the gene might affect the expression in these samples (11, 12). However, we consider that the genomic loss of *CDKN2A* has a greater influence on the expression of the gene than the methylation because the CDKN2A expression levels were remarkably reduced in accordance with the genomic loss (Fig. 2B and D).

Alterations of both *CDKN2A* and *TP53* were previously reported to be mutually exclusive (34), and our results showed the same trend. In addition, loss of *TP53* and gains of *MDM4*/*RFWD2* tended to be mutually exclusive in our acute-type ATL samples. Because these genes are involved in the TP53 pathway, our findings indicate that the TP53 pathway may also play a pivotal role in the pathophysiology of acute-type ATL. In fact, 80% of acute-type ATL had the alterations of cell-cycle–related genes, including *CDKN2A* and *TP53*. On the basis of this finding, we found that the alterations of cell-cycle–related genes might be predictive factors for acute transformation in chronic-type ATL cases (Fig. 5B).

Disruption of the immunosurveillance system in acute transformation of chronic-type ATL

The combined analyses of aCGH and sequencing revealed that 19% of ATL cases (7% of chronic-type and 29% of acute-type ATL) exhibited the *CD58* alteration. One acute-type ATL case showed somatic mutation, and the other cases showed genomic loss of the *CD58* locus. The alteration of *B2M* was a rare event in ATL compared with DLBCL (20). CD58 is a ligand of the CD2 receptor that is expressed on CTLs and NK cells and contributes to adhesion and activation of these cells. Previous reports showed that CTLs and NK cells could not recognize and injure target cells when treated with monoclonal CD58 antibody (35, 36). It is important to note that immune escape mechanism by CD58 inactivation was proven in DLBCL by Challa-Malladi and colleagues (20). The genomic loss and nonsense mutation of CD58 were for the first time demonstrated in ATL in this study and were suggested to be a predictive marker for acute transformation in chronic-type ATL. Therefore, the immune escape mechanism by the CD58 inactivation is likely to be involved in the pathophysiology of ATL as shown in DLBCL although detailed analysis is needed in the future.

Administration of immunosuppressive drugs to HTLV-1 carriers is currently considered a risk factor for early development of ATL (37, 38). It has been also suggested that immune escape from CTLs is induced by inactivation of the Tax protein derived from HTLV-1 in ATL (39–41). In addition, a report also suggested that immune escape from NK cells played an important role in ATL development (42). These findings suggest the presence of an immune escape mechanism in the pathophysiology of ATL. The present result regarding the significance of *CD58* alteration as a predictive factor for acute transformation in chronic-type ATL should be validated in more number of cases in the future study. Further studies are also needed regarding the protein expressions of CD58, B2M, and human leukocyte antigen class I.

In conclusion, our comparison of the molecular characteristics of chronic-type and acute-type ATL revealed that deregulation of the cell cycle and escape from the immune system are likely to be involved in acute transformation of chronic-type ATL. Development of ATL is thought to involve accumulation of several genomic alterations (43). The alterations of both pathways discovered in this study might be the late events following viral infection in the pathophysiology of ATL. These alterations could serve as biomarkers for patients with

chronic-type ATL. Furthermore, the presence of genomic alterations related to immune escape should be considered in the development of immunotherapeutic approaches for ATL.

Disclosure of Potential Conflicts of Interest

No potential conflicts of interest were disclosed.

Authors' Contributions

Conception and design: N. Yoshida, A. Utsunomiya, K. Tsukasaki, A. Umino, M. Seto

Development of methodology: K. Karube

Acquisition of data (provided animals, acquired and managed patients, provided facilities, etc.): N. Yoshida, A. Utsunomiya, K. Tsukasaki, Y. Imaizumi, N. Taira, K. Arita, S. Tsuzuki, K. Ohshima

Analysis and interpretation of data (e.g., statistical analysis, biostatistics, computational analysis): N. Yoshida, A. Utsunomiya, K. Arita, M. Suguro, S. Tsuzuki

Writing, review, and/or revision of the manuscript: N. Yoshida, K. Karube, A. Utsunomiya, K. Tsukasaki, T. Kinoshita, M. Seto

Administrative, technical, or material support (i.e., reporting or organizing data, constructing databases): A. Utsunomiya, N. Uike, T. Kinoshita, M. Seto

Study supervision: K. Karube, M. Seto

Acknowledgments

The outstanding technical assistance of Yumiko Kasugai, Seiko Sato, and Kyoko Hirano is very much appreciated. The authors thank Drs. Takashi Miyagi, Sivasundaram Karnan, Harumi Kato, Kiyoko Yamamoto, Fang Liu, Tatsuo Kakiuchi, and Taishi Takahara for their critical discussions and constructive suggestions. N. Yoshida also thanks Drs. Akira Sakai, Yuta Katayama, Hideki Asaoku, and Tatsuo Ichinohe for their encouragement throughout this study.

Grant Support

This work was supported in part by a grant-in-Aid from the Ministry of Health, Labor and Welfare of Japan, the Ministry of Education, Culture, Sports, Science and Technology of Japan, the Japan Society for the Promotion of Science (N. Yoshida, K. Karube, S. Tsuzuki, and M. Seto), a grant-in-Aid for Cancer Research from the Ministry of Health, Labor and Welfare of Japan (M. Seto), and a grant-in-Aid from the Takeda Science Foundation (M. Seto).

The costs of publication of this article were defrayed in part by the payment of page charges. This article must therefore be hereby marked *advertisement* in accordance with 18 U.S.C. Section 1734 solely to indicate this fact.

Received March 6, 2014; revised June 30, 2014; accepted July 22, 2014; published OnlineFirst October 15, 2014.

References

1. Uchiyama T, Yodoi J, Sagawa K, Takatsuki K, Uchino H. Adult T-cell leukemia: clinical and hematologic features of 16 cases. Blood 1977;50:481–92.
2. Ohshima K, Jaffe E, Kikuchi M. Adult T-cell leukemia/lymphoma. In: Swerdlow SH CE, Harris NL, Jaffe ES, Pileri SA, Stein H, Thiele J, Vardiman JW, editors. World Health Organization classification of tumours: pathology and genetics of tumours of haematopoietic and lymphoid tissues pathology and genetics of tumours of haematopoietic and lymphoid tissues 4th ed. Lyon, France: IARC Press; 2009. p. 281–4.
3. Shimoyama M. Diagnostic criteria and classification of clinical subtypes of adult T-cell leukaemia-lymphoma. A report from the Lymphoma Study Group (1984–87). Br J Haematol 1991;79:428–37.
4. Takasaki Y, Iwanaga M, Imaizumi Y, Tawara M, Joh T, Kohno T, et al. Long-term study of indolent adult T-cell leukemia-lymphoma. Blood 2010;115:4337–43.
5. Tsukasaki K, Hermine O, Bazarbachi A, Ratner L, Ramos JC, Harrington W Jr, et al. Definition, prognostic factors, treatment, and response criteria of adult T-cell leukemia-lymphoma: a proposal from an international consensus meeting. J Clin Oncol 2009;27:453–9.
6. Sakashita A, Hattori T, Miller CW, Suzushima H, Asou N, Takatsuki K, et al. Mutations of the p53 gene in adult T-cell leukemia. Blood 1992;79:477–80.
7. Hatta Y, Hirama T, Miller CW, Yamada Y, Tomonaga M, Koeffler HP. Homozygous deletions of the p15 (MTS2) and p16 (CDKN2/MTS1) genes in adult T-cell leukemia. Blood 1995;85:2699–704.
8. Nishimura S, Asou N, Suzushima H, Okubo T, Fujimoto T, Osato M, et al. p53 gene mutation and loss of heterozygosity are associated with increased risk of disease progression in adult T cell leukemia. Leukemia 1995;9:598–604.
9. Uchida T, Kinoshita T, Watanabe T, Nagai H, Murate T, Saito H, et al. The CDKN2 gene alterations in various types of adult T-cell leukaemia. Br J Haematol 1996;94:665–70.
10. Yamada Y, Hatta Y, Murata K, Sugawara K, Ikeda S, Mine M, et al. Deletions of p15 and/or p16 genes as a poor-prognosis factor in adult T-cell leukemia. J Clin Oncol 1997;15:1778–85.
11. Trovato R, Cereseto A, Takemoto S, Gessain A, Watanabe T, Waldmann T, et al. Deletion of the p16INK4A gene in ex vivo acute adult T cell lymphoma/leukemia cells and methylation of the p16INK4A promoter in HTLV type I-infected T cell lines. AIDS Res Hum Retroviruses 2000;16:709–13.
12. Nosaka K, Maeda M, Tamiya S, Sakai T, Mitsuya H, Matsuoka M. Increasing methylation of the CDKN2A gene is associated with the progression of adult T-cell leukemia. Cancer Res 2000;60:1043–8.
13. Tsukasaki K, Krebs J, Nagai K, Tomonaga M, Koeffler HP, Bartram CR, et al. Comparative genomic hybridization analysis in adult T-cell leukemia/lymphoma: correlation with clinical course. Blood 2001;97:3875–81.
14. Umino A, Nakagawa M, Utsunomiya A, Tsukasaki K, Taira N, Katayama N, et al. Clonal evolution of adult T-cell leukemia/lymphoma takes place in the lymph nodes. Blood 2011;117:5473–8.
15. Karube K, Nakagawa M, Tsuzuki S, Takeuchi I, Honma K, Nakashima Y, et al. Identification of FOXO3 and PRDM1 as tumor-suppressor gene candidates in NK-cell neoplasms by genomic and functional analyses. Blood 2011;118:3195–204.
16. Yoshida N, Nishikori M, Izumi T, Imaizumi Y, Sawayama Y, Niino D, et al. Primary peripheral T-cell lymphoma, not otherwise specified of the thyroid with autoimmune thyroiditis. Br J Haematol 2013;161:214–23.
17. Pasqualucci L, Trifonov V, Fabbri G, Ma J, Rossi D, Chiarenza A, et al. Analysis of the coding genome of diffuse large B-cell lymphoma. Nat Genet 2011;43:830–7.
18. Subramanian A, Tamayo P, Mootha VK, Mukherjee S, Ebert BL, Gillette MA, et al. Gene set enrichment analysis: a knowledge-based approach for interpreting genome-wide expression profiles. Proc Natl Acad Sci U S A 2005;102:15545–50.
19. Palomero T, Couronne L, Khiabanian H, Kim MY, Ambesi-Impiombato A, Perez-Garcia A, et al. Recurrent mutations in epigenetic regulators, RHOA and FYN kinase in peripheral T cell lymphomas. Nat Genet 2014;46:166–70.
20. Challa-Malladi M, Lieu YK, Califano O, Holmes AB, Bhagat G, Murty VV, et al. Combined genetic inactivation of beta2-Microglobulin and CD58 reveals frequent escape from immune recognition in diffuse large B cell lymphoma. Cancer Cell 2011;20:728–40.
21. Kanda Y. Investigation of the freely available easy-to-use software 'EZR' for medical statistics. Bone Marrow Transplant 2013;48:452–8.
22. Lenz G, Wright GW, Emre NC, Kohlhammer H, Dave SS, Davis RE, et al. Molecular subtypes of diffuse large B-cell lymphoma arise by distinct genetic pathways. Proc Natl Acad Sci U S A 2008;105:13520–5.
23. Honma K, Tsuzuki S, Nakagawa M, Tagawa H, Nakamura S, Morishima Y, et al. TNFAIP3/A20 functions as a novel tumor suppressor gene in several subtypes of non-Hodgkin lymphomas. Blood 2009;114:2467–75.
24. Monti S, Chapuy B, Takeyama K, Rodig SJ, Hao Y, Yeda KT, et al. Integrative analysis reveals an outcome-associated and targetable pattern of p53 and cell cycle deregulation in diffuse large B cell lymphoma. Cancer Cell 2012;22:359–72.

25. Kanner SB, Damle NK, Blake J, Aruffo A, Ledbetter JA. CD2/LFA-3 ligation induces phospholipase-C gamma 1 tyrosine phosphorylation and regulates CD3 signaling. J Immunol 1992;148:2023–9.
26. Wang JH, Smolyar A, Tan K, Liu JH, Kim M, Sun ZY, et al. Structure of a heterophilic adhesion complex between the human CD2 and CD58 (LFA-3) counterreceptors. Cell 1999;97:791–803.
27. Martelli MP, Lin H, Zhang W, Samelson LE, Bierer BE. Signaling via LAT (linker for T-cell activation) and Syk/ZAP70 is required for ERK activation and NFAT transcriptional activation following CD2 stimulation. Blood 2000;96:2181–90.
28. Salmond RJ, Filby A, Qureshi I, Caserta S, Zamoyska R. T-cell receptor proximal signaling via the Src-family kinases, Lck and Fyn, influences T-cell activation, differentiation, and tolerance. Immunol Rev 2009;228:9–22.
29. Mizutani A, Fukuda M, Ibata K, Shiraishi Y, Mikoshiba K. SYNCRIP, a cytoplasmic counterpart of heterogeneous nuclear ribonucleoprotein R, interacts with ubiquitous synaptotagmin isoforms. J Biol Chem 2000;275:9823–31.
30. Egan JB, Thompson PA, Ashbeck EL, Conti DV, Duggan D, Hibler E, et al. Genetic polymorphisms in vitamin D receptor VDR/RXRA influence the likelihood of colon adenoma recurrence. Cancer Res 2010;70:1496–504.
31. Chigrinova E, Rinaldi A, Kwee I, Rossi D, Rancoita PM, Strefford JC, et al. Two main genetic pathways lead to the transformation of chronic lymphocytic leukemia to Richter syndrome. Blood 2013;122:2673–82.
32. Fabbri G, Khiabanian H, Holmes AB, Wang J, Messina M, Mullighan CG, et al. Genetic lesions associated with chronic lymphocytic leukemia transformation to Richter syndrome. J Exp Med 2013;210:2273–88.
33. Yamagishi M, Nakano K, Miyake A, Yamochi T, Kagami Y, Tsutsumi A, et al. Polycomb-mediated loss of miR-31 activates NIK-dependent NF-kappaB pathway in adult T cell leukemia and other cancers. Cancer Cell 2012;21:121–35.
34. Tawara M, Hogerzeil SJ, Yamada Y, Takasaki Y, Soda H, Hasegawa H, et al. Impact of p53 aberration on the progression of Adult T-cell Leukemia/Lymphoma. Cancer Lett 2006;234:249–55.
35. Altomonte M, Gloghini A, Bertola G, Gasparollo A, Carbone A, Ferrone S, et al. Differential expression of cell adhesion molecules CD54/CD11a and CD58/CD2 by human melanoma cells and functional role in their interaction with cytotoxic cells. Cancer Res 1993;53:3343–8.
36. Gwin JL, Gercel-Taylor C, Taylor DD, Eisenberg B. Role of LFA-3, ICAM-1, and MHC class I on the sensitivity of human tumor cells to LAK cells. J Surg Res 1996;60:129–36.
37. Kawano N, Shimoda K, Ishikawa F, Taketomi A, Yoshizumi T, Shimoda S, et al. Adult T-cell leukemia development from a human T-cell leukemia virus type I carrier after a living-donor liver transplantation. Transplantation 2006;82:840–3.
38. Yoshizumi T, Shirabe K, Ikegami T, Kayashima H, Yamashita N, Morita K, et al. Impact of human T cell leukemia virus type 1 in living donor liver transplantation. Am J Transplant 2012;12:1479–85.
39. Kannagi M, Harashima N, Kurihara K, Ohashi T, Utsunomiya A, Tanosaki R, et al. Tumor immunity against adult T-cell leukemia. Cancer Sci 2005;96:249–55.
40. Matsuoka M. Human T-cell leukemia virus type I (HTLV-I) infection and the onset of adult T-cell leukemia (ATL). Retrovirology 2005;2:27.
41. Suzuki S, Masaki A, Ishida T, Ito A, Mori F, Sato F, et al. Tax is a potential molecular target for immunotherapy of adult T-cell leukemia/lymphoma. Cancer Sci 2012;103:1764–73.
42. Stewart SA, Feuer G, Jewett A, Lee FV, Bonavida B, Chen IS. HTLV-1 gene expression in adult T-cell leukemia cells elicits an NK cell response in vitro and correlates with cell rejection in SCID mice. Virology 1996;226:167–75.
43. Okamoto T, Ohno Y, Tsugane S, Watanabe S, Shimoyama M, Tajima K, et al. Multi-step carcinogenesis model for adult T-cell leukemia. Jpn J Cancer Res 1989;80:191–5.

OPEN ACCESS Freely available online

PLOS ONE

Detection of the G17V RHOA Mutation in Angioimmunoblastic T-Cell Lymphoma and Related Lymphomas Using Quantitative Allele-Specific PCR

Rie Nakamoto-Matsubara[1], Mamiko Sakata-Yanagimoto[1,2,3], Terukazu Enami[1], Kenichi Yoshida[4], Shintaro Yanagimoto[5], Yusuke Shiozawa[4], Tohru Nanmoku[6], Kaishi Satomi[7], Hideharu Muto[1,2,3], Naoshi Obara[1,2,3], Takayasu Kato[1,2,3,8], Naoki Kurita[1,2,3], Yasuhisa Yokoyama[1,2,3], Koji Izutsu[9,10], Yasunori Ota[11], Masashi Sanada[4], Seiichi Shimizu[3,12], Takuya Komeno[3,13], Yuji Sato[14], Takayoshi Ito[15], Issay Kitabayashi[16], Kengo Takeuchi[17], Naoya Nakamura[18], Seishi Ogawa[4], Shigeru Chiba[1,2,3,8]*

1 Department of Hematology, Graduate School of Comprehensive Human Sciences, University of Tsukuba, Tsukuba, Ibaraki, Japan, **2** Department of Hematology, Faculty of Medicine, University of Tsukuba, Tsukuba, Ibaraki, Japan, **3** Department of Hematology, University of Tsukuba Hospital, Tsukuba, Ibaraki, Japan, **4** Department of Pathology and Tumor Biology, Graduate School of Medicine, Kyoto University, Sakyo-ku, Kyoto, Japan, **5** Division for Health Service Promotion, The University of Tokyo, Bunkyo-ku, Tokyo, Japan, **6** Department of Clinical Laboratory, University of Tsukuba Hospital, Tsukuba, Ibaraki, Japan, **7** Department of Pathology, University of Tsukuba Hospital, Tsukuba, Ibaraki, Japan, **8** Life Science Center, Tsukuba Advanced Research Center, University of Tsukuba, Tsukuba, Ibaraki, Japan, **9** Department of Hematology, Toranomon Hospital, Minato-ku, Tokyo, Japan, **10** Okinaka Memorial Institute for Medical Research, Minato-ku, Tokyo, Japan, **11** Department of Pathology, Toranomon Hospital, Minato-ku, Tokyo, Japan, **12** Department of Hematology, Tsuchiura Kyodo General Hospital, Tsuchiura, Ibaraki, Japan, **13** Department of Hematology, Mito Medical Center, National Hospital Organization, Ibaraki-machi, Ibaraki, Japan, **14** Department of Hematology, Tsukuba Memorial Hospital, Tsukuba, Ibaraki, Japan, **15** Department of Hematology, JA Toride Medical Center, Toride, Ibaraki, Japan, **16** Division of Hematological Malignancy, National Cancer Center Research Institute, Chuo-ku, Tokyo, Japan, **17** Pathology Project for Molecular Targets, The Cancer Institute, Japanese Foundation for Cancer Research, Koto-ku, Tokyo, Japan, **18** Department of Pathology, Tokai University School of Medicine, Isehara, Kanagawa, Japan

Abstract

Angioimmunoblastic T-cell lymphoma (AITL) and peripheral T-cell lymphoma, not otherwise specified (PTCL-NOS) are subtypes of T-cell lymphoma. Due to low tumor cell content and substantial reactive cell infiltration, these lymphomas are sometimes mistaken for other types of lymphomas or even non-neoplastic diseases. In addition, a significant proportion of PTCL-NOS cases reportedly exhibit features of AITL (AITL-like PTCL-NOS). Thus disagreement is common in distinguishing between AITL and PTCL-NOS. Using whole-exome and subsequent targeted sequencing, we recently identified G17V *RHOA* mutations in 60–70% of AITL and AITL-like PTCL-NOS cases but not in other hematologic cancers, including other T-cell malignancies. Here, we establish a sensitive detection method for the G17V *RHOA* mutation using a quantitative allele-specific polymerase chain reaction (qAS-PCR) assay. Mutated allele frequencies deduced from this approach were highly correlated with those determined by deep sequencing. This method could serve as a novel diagnostic tool for 60–70% of AITL and AITL-like PTCL-NOS.

Citation: Nakamoto-Matsubara R, Sakata-Yanagimoto M, Enami T, Yoshida K, Yanagimoto S, et al. (2014) Detection of the G17V RHOA Mutation in Angioimmunoblastic T-Cell Lymphoma and Related Lymphomas Using Quantitative Allele-Specific PCR. PLoS ONE 9(10): e109714. doi:10.1371/journal.pone.0109714

Editor: Kristy L. Richards, University of North Carolina at Chapel Hill, United States of America

Received March 27, 2014; **Accepted** September 4, 2014; **Published** October 13, 2014

Data Availability: The authors confirm that all data underlying the findings are fully available without restriction. All relevant data are within the paper and its Supporting Information files.

Funding: This work was supported by Grants-in-Aid for Scientific Research (KAKENHI) (24390241, 23659482, 23118503, and 22130002 to S.C.; 25461407 to M.S.-Y.), and the Adaptable and Seamless Technology Transfer Program through target-driven R and D (A-STEP) to M.S.-Y. from the Ministry of Education, Culture, Sports, Science and Technology of Japan. This work was also supported by the Mochida Memorial Foundation for Medical and Pharmaceutical Research, and the Uehara Memorial Foundation to M.S.-Y. The funders had no role in study design, data collection and analysis, decision to publish, or preparation of the manuscript.

Competing Interests: The authors have declared that no competing interests exist.

* Email: schiba-tky@umin.net

Introduction

Based on the classification proposed by the World Health Organization (WHO), Angioimmunoblastic T-cell lymphoma (AITL) is a distinct subtype of T-cell lymphoma that accounts for 20% of peripheral T-cell lymphoma cases [1]. AITL is characterized by generalized lymphadenopathy, hyperglobulinemia, and autoimmune-like manifestations [1,2]. Pathologic examination of AITL tumors reveals polymorphous infiltration of reactive cells, including endothelial venules and follicular dendritic cells [3,4]. Based on gene expression profiling and immunohistochemical staining, the normal counterparts of AITL tumor cells are proposed to be follicular helper T cells (TFHs) [5]. Peripheral T-cell lymphoma, not otherwise specified (PTCL-NOS) is a more heterogenous type of lymphoma, one that shows variation even in CD4 and CD8 expression. Some PTCL-NOS cases share features of AITL, such as immunohistochemical

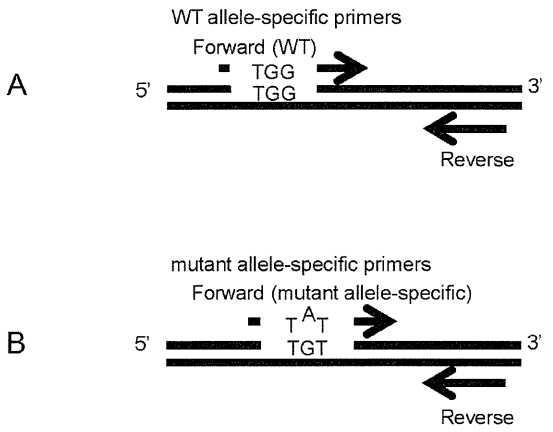

Figure 1. Design of primers used in the study. A WT allele-specific primer forward primer (Upper), a mutant allele-specific forward primer (Lower), and a common primer were designed. The 3′ end of the forward mutant primer was specific to the mutant site (G to T) and an internal mismatch at the second nucleotide from 3′ end (G to A) was introduced to improve specificity.
doi:10.1371/journal.pone.0109714.g001

staining patterns resembling those seen in AITL (AITL-like PTCL-NOS) [6].

Expertise is required to diagnose AITL and PTCL-NOS because generally low tumor cell content obscures the neoplastic nature of some cases, and large reactive B-cells are often confused with tumor cells [7]. Clonal rearrangement of the T-cell receptor gene is undetectable in 10–25% of AITL cases due to low tumor cell frequency [1]. In addition, clonal growth of Epstein-Bar virus-infected B-cells is not uncommon in these kinds of cancers, causing detection of clonal immunoglobulin gene rearrangement in 20% of these case. [1].

Mutations in *TET2, IDH2*, and *DNMT3A* are frequently seen in AITL and AITL-like PTCL-NOS [8,9], although these mutations are also common to various myeloid malignancies [10,11]. We and others reported a large cohort of AITL and PTCL-NOS patients revealing that the G17V *RHOA* mutation was highly specific to AITL and AITL-like PTCL-NOS and very frequent (seen in 60–70% of cases) in these T-cell lymphomas [12,13]. This observation suggests that detection of the G17V *RHOA* mutation could serve as a new diagnostic tool to discriminate these lymphomas from other diseases. One difficulty, however, is that *RHOA* mutation allele frequencies in these lymphomas are generally as low as <0.2 or often <0.1, reflecting low tumor cell content. Therefore, diagnosis of these conditions requires development of sensitive and cost-efficient methods that are as accurate as deep sequencing, which is expensive and not commonly used in most clinical testing facilities.

To meet this need, we developed a quantitative allele-specific polymerase chain reaction (qAS-PCR) method that sensitively detects the G17V *RHOA* mutation in a highly accurate manner. This assay should provide a realistic way to conduct laboratory testing to diagnose AITL and AITL-like PTCL-NOS.

Materials and Methods

Primer design

We designed two forward primers that discriminate wild-type (WT) from G17V *RHOA* for use with one common reverse primer. The mutant forward primer was designed using a previously described algorithm [14]. The 3′ end is specific to the mutant site and an internal mismatch at the second nucleotide from the 3′ end was introduced to improve specificity (Figure 1 and Table 1). We performed local alignment analysis using the BLAST program (http://www.ncbi.nlm.nih.gov/tools/primer-blast/) to confirm primer specificity.

Preparation of plasmids containing WT and mutant cDNA and standard curve generation

WT or G17V mutant *RHOA* cDNA was subcloned into pBluescript (pBS/wtRHOA or pBS/mutRHOA, respectively; Agilent Technologies, Santa Clara, CA). qPCR reactions were performed in a final volume of 20 μl using 10 nM primers and the SYBR-Green mix (Roche Applied Science, Mannheim, Germany), and amplicons were subjected to either the ABI7500 or 7900 Fast Sequence Detection Systems (Life Technologies, Carlsbad, CA). Use of either the WT or mutant forward primer plus the common primer generated a 73-bp PCR product. The following PCR conditions were used: 10 min at 95°C, followed by 40 cycles of 15 sec at 95°C and 60 sec at 60°C.

Standard curves of amplicon levels were created by qPCR using serially-diluted pBS/wtRHOA or pBS/mutRHOA with WT or mutant primers, respectively.

Preparation of template plasmid DNA mixtures

pBS/mutRHOA was mixed with pBS/wtRHOA in 100, 10, 1.0, 0.1, 0.01 and 0% ratios. Overall DNA concentration was adjusted to 1.0 ng/well of a plate. All mixtures were then serially-diluted 1:10 for 4 cycles. qPCR was performed with these templates plus primers using conditions described above.

Patients and samples

Tumor samples were collected from 53 patients with AITL, 55 with PTCL-NOS, 19 with B-cell malignancies, 129 with myeloid malignancies, and 5 with another T-cell lymphoma (for a total of 261), according to WHO classification. Twenty-seven non-tumor samples, including bone marrow mononuclear cells and buccal cells from lymphoma patients, were also analyzed as controls. The Ethics Committee University of Tsukuba Hospital approved the protocol and consent procedure, according to which written informed consent was provided by the participants. Genomic DNA was extracted from 13 formalin-fixed/paraffin-

Table 1. Sequence of allele-specific primers used for this study.

Primer	Sequence
Forward (WT*[1])	ATTGTTGGTGATGGAGCCTGTGG
Forward (MUT*[2])	ATTGTTGGTGATGGAGCCTGTAT
Reverse (common)	ACACCTCTGGGAACTGGTCCT

*[1] WT, wild-type; *[2] MUT, mutant.
doi:10.1371/journal.pone.0109714.t001

Table 2. Analysis of genomic DNA samples.

Disease	Frozen amp*[1]	Frozen not-amp*[2]	PLP not-amp	FFPE not-amp	Total
AITL	14	10	19	10	53
PTCL-NOS	16	8	28	3	55
B-cell lymphoma	1	18			19
Myeloid malignancies	129				129
Other T-cell lymphomas		5			5
Control samples	27				27
Total	187	41	47	13	288

*[1]amp, amplified; *[2]not-amp, not-amplified.

doi:10.1371/journal.pone.0109714.t002

embedded (FFPE), 47 periodate/lysine/paraformaldehyde (PLP)-fixed, and 228 fresh frozen specimens, using an FFPE tissue kit (QIAGEN, Hilden, Germany) for FFPE and PLP samples and a Puregene DNA blood kit (QIAGEN) for fresh frozen specimens, according to manufacturer's instructions.

One hundred and one DNA samples were original, while 187 were whole genome-amplified by either GenomiPhi (GE, Fairfield, CT) or a RepliG mini kit (Qiagen) (Table 2). For DNA extracted from FFPE samples, we also prepared PCR amplicon with AmpliTaq Gold 360 (Life technologies) in a final volume of 20 μl with 20 ng genomic DNA, 5 nM primers (Table 3), 5 μl of AmpliTaq gold master mix, and 0.3 μl of 360 GC Enhancer. For this amplicon preparation, the following PCR conditions were used: one cycle of 15 min at 95°C, 4 min at 60°C, and 1 min at 72°C, next 35 cycles of 1 min at 95°C, 1 min at 60°C, and 1 min at 72°C, and finally 10 min at 72°C and kept at 4°C. Amplicons were purified using PCR purification kit (QIAGEN).

Each DNA sample was quantified using the Qubit dsDNA HS Assay kit and a Qubit fluorometer (Life Technologies, Carlsbad, CA). Extracted DNA samples were stored at −20°C until use.

For 108 of the total 288 genomic DNA samples, data sets for mutant allele frequencies obtained by deep sequencing using the MiSeq System (Illumina, San Diego, CA), which were used in our previous report [12], were reanalyzed.

qPCR of patient samples

qPCR reactions using duplicate patient samples were performed in a final volume of 20 μl with 50 ng of original or whole genome-amplified genomic DNA or 1.0×10^{-2} ng PCR-amplified DNA as a template, 10 nM primers, and the SYBR-Green mix (Roche, Basel, Switzerland) in conditions similar to those used for plasmid templates described above.

Levels of amplicons generated using either the WT or mutant primer, calculated with reference to respective standard curves, were designated [wt] and [mut], respectively.

Table 3. Primer sequences for making PCR amplicons of FFPE samples.

Primer	Sequence
Forward	GCCCCATGGTTACCAAAGCA
Reverse	GCTTTCCATCCACCTCGATA

doi:10.1371/journal.pone.0109714.t003

Statistical analysis

Statistical analysis was conducted using SPSS software (Japan International Business.

Machines Corporation, Tokyo). A P-value <0.05 was considered statistically significant.

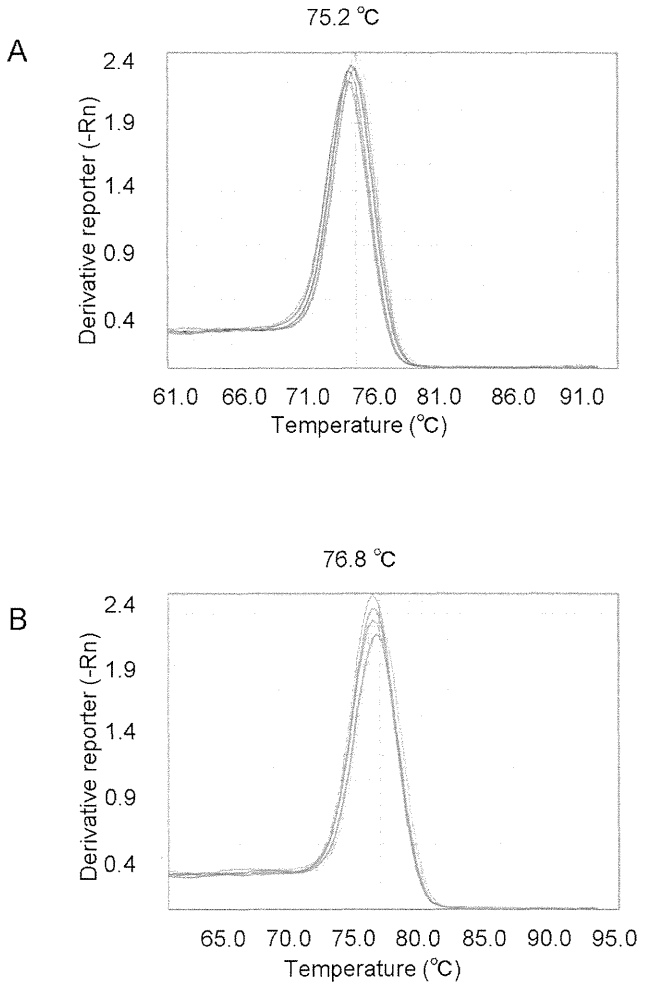

Figure 2. Melting curve analysis. A. Melting curve constructed using WT allele-specific primers. B. Melting curve constructed using mutant allele-specific primer set.

doi:10.1371/journal.pone.0109714.g002

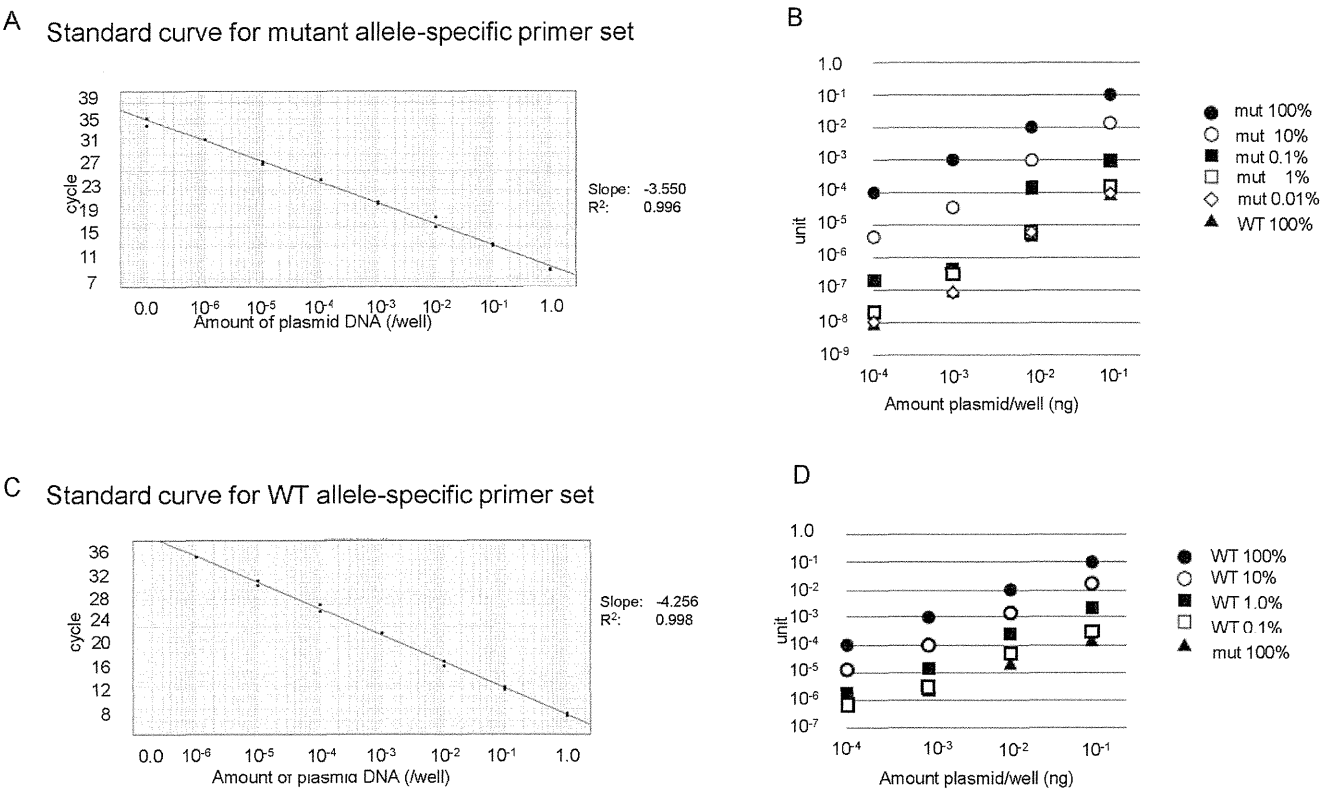

Figure 3. Standard curve showing linearity of quantitative allele-specific PCR. A standard curve was generated by serial dilution of WT or G17V cDNA that had been subcloned into pBluescript. A. Serial dilution of pBS/mutRHOA. Black dots correspond to 1.0×10^{-9}~1.0 unit of mutant plasmid (duplicate samples). The titration slope is −3.550 and R^2 is 0.996. B. pBS/mutRHOA was mixed with pBS/wtRHOA at 100%, 10%, 1.0%, 0.1%, 0.01% and 0%. Mix concentrations were adjusted to 1.0 ng/well and diluted 1:10 4 times for quantitative PCR analysis with allele-specific mutant primers. Horizonal axis indicates the amount of DNA per well. Vertical axis indicates unit for each sample. Black dot, MUT 100%; open dot, MUT 10%; square, MUT 1%; open square, MUT 0.1%; diamond, MUT 0.01%; triangle, MUT 0% (WT 100%) C. Serial dilution of pBS/wtRHOA. Black dots correspond to 1.0×10^{-6}~1.0 unit of WT cDNA (duplicate samples). The titration slope is −4.256, and R^2 is 0.998. D. pBS/wtRHOA was mixed with pBS/mutRHOA at 100%, 10%, 1.0%, 0.1%, 0.1% and 0%. Mix concentrations were adjusted to 1.0 ng/well and diluted 1:10 4 times for quantitative PCR analysis with WT allele-specific primers. Black dot, WT 100%; open dot, WT 10%; square, WT 1%; open square, WT 0.1%; triangle, WT 0% (MUT 100%).
doi:10.1371/journal.pone.0109714.g003

Results

Primer specificity

Melting curve analysis revealed that amplicons generated using either WT or mutant primers melted at 76.8°C or 75.3°C, respectively. Non-specific amplicons were not observed in either pBS/wtRHOA/WT primer or pBS/mutRHOA/mutant primer combinations (Figures 2A and 2B).

Linearity of amplicon generation

We then varied either the ratio of pBS/mutRHOA to pBS/wtRHOA or the concentration of total input DNA, and measured the amounts of PCR product generated using the mutant primer. Because we observed a nearly linear relationship between the amounts of generated amplicon and input DNA in the range of 10^4 (1–0.0001 ng DNA/well) at each ratio of pBS/mutRHOA to pBS/wtRHOA (Figure 3A), we defined the amount of amplicon derived from 100% pBS/mutRHOA template at 0.1 ng/well as 0.1 unit, and tested whether linearity was maintained with varying ratios of pBS/mutRHOA to pBS/wtRHOA. The template samples of 0.1 ng/well containing 10, 1, 0.1, and 0.01% pBS/mutRHOA were measured as 1.0×10^{-2} unit (C.I. (confidence interval), $0.8–1.3\times10^{-2}$; S.F. (scaling factor), 0.95–1.06), 1.2×10^{-3} unit (C.I., $0.8–1.6\times10^{-3}$; S.F., 0.96–1.07), 2.2×10^{-4} unit (C.I., $1.5–3.0\times10^{-4}$; S.F., 1.05–1.14), and 1.0×10^{-5} unit (C.I., $0.4–1.6\times10^{-5}$; S.F., 0.92–1.04), indicative of linearity in the range of 10^4 (100–0.01%). Taken together, linearity was maintained in the range of 10^9 (Figures 3A and 3B).

Similarly, when we assessed the WT primer using various ratios of pBS/wtRHOA to pBS/mutRHOA and concentrations of input DNA, linearity between the amounts of amplicon and template were maintained between 100–0.1% (a range of 10^3) and 1–0.001 ng DNA/well (a range of 10^3). This analysis indicated a total dynamic range of 10^6 (Figures 3C and 3D).

qAS-PCR of T-cell lymphoma samples

qAS-PCR with 50 ng of genomic DNA was performed using 106 AITL and PTCL-NOS samples including 11 FFPE samples. The [wt] and [mut] values were distributed between 7.9×10^{-5} and 1.8×10^{-1} units, and 2.0×10^{-7} and 7.6×10^{-2} units, respectively. Nevertheless, it was not possible to use absolute values of [mut] for levels of G17V *RHOA* alleles, due to variation in DNA quality. Therefore, we undertook relative measures to assess G17V *RHOA* allele frequency. To do so, we calculated a [mut]/([wt]+[mut]) value and compared it with mutant variant allele frequencies determined by MiSeq. [mut]/([wt]+[mut]) values were distributed between 3.2×10^{-4} and 3.0×10^{-1}. Among samples judged to harbor a G17V *RHOA* mutation by deep sequencing using the MiSeq System (cut-off level, 0.02), which was defined in previous paper [12], [mut]/([wt]+[mut]) values of DNA

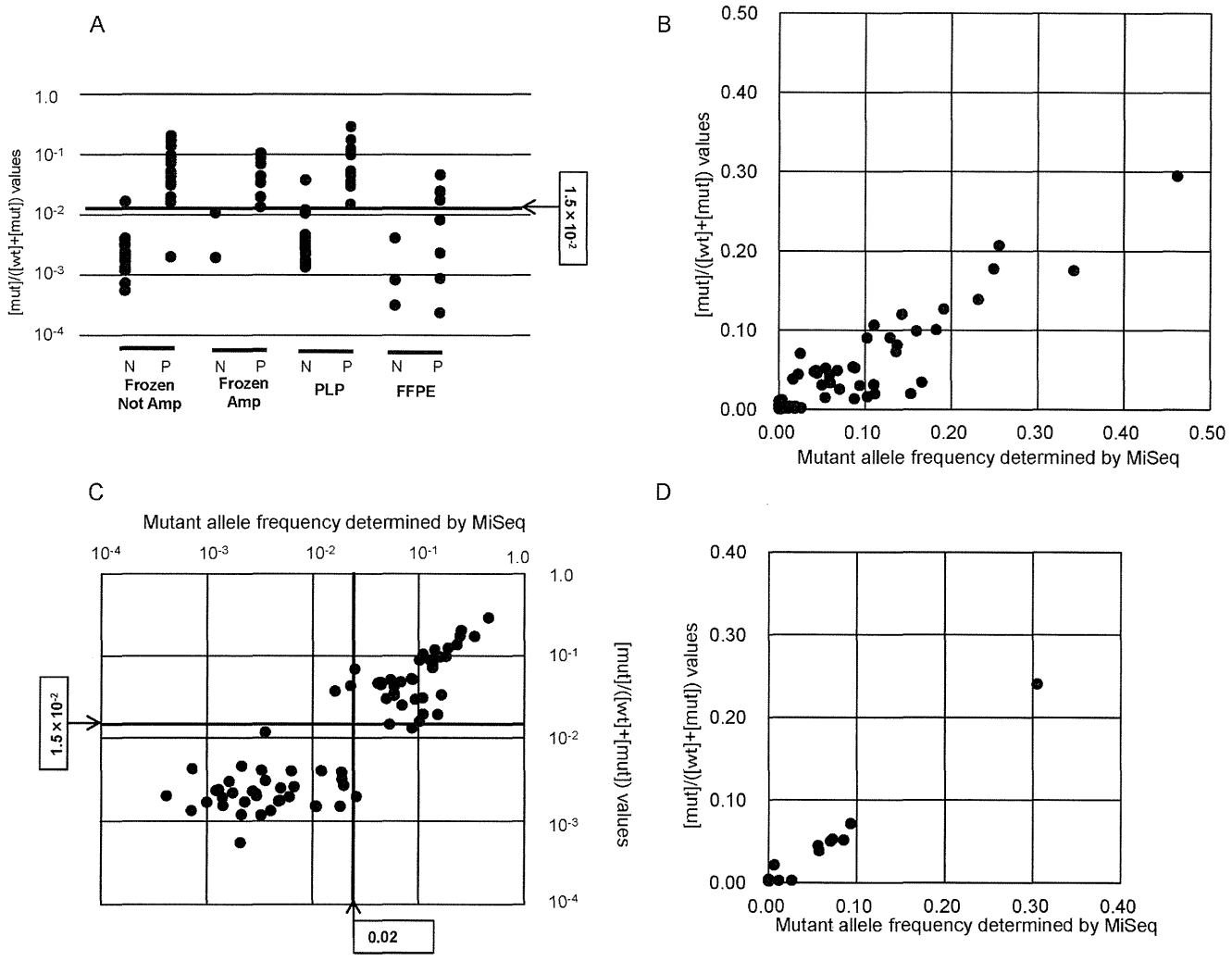

Figure 4. qAS-PCR of AITL and PTCL-NOS samples. A, Shown are [mut]/([wt]+[mut]) values for each sample. N, mutation negative determined by MiSeq; P, mutation positive determined by MiSeq; Amp, amplified; PLP, periodate/lysine/paraformaldehyde-fixed; FFPE, formalin-fixed/paraffin-embedded. B, Comparison of [mut]/([wt]+[mut]) values by qAS-PCR and mutant allele frequencies as determined by MiSeq for 95 original or whole genome-amplified DNA samples, including 43 AITL and 52 PTCL-NOS. Cut-off values were determined as 1.5×10^{-2} for [mut]/([wt]+[mut]) by qAS-PCR and as 0.02 for mutant allele frequencies as determined by MiSeq. C, Comparison of [mut]/([wt]+[mut]) values by qAS-PCR and mutant allele frequencies as determined by MiSeq for 95 DNA samples in a log scales. D, Comparison of [mut]/([wt]+[mut]) values by qAS-PCR and mutant allele frequencies as determined by MiSeq for 13 FFPE PCR-amplicon samples.
doi:10.1371/journal.pone.0109714.g004

from MiSeq-positive FFPE samples were significantly lower than those from other MiSeq-positive samples (Miseq-positive FFPE vs MiSeq-positive other samples; 1.56×10^{-2} vs. 9.38×10^{-2}, $p<0.05$, Student's t-test) (Figure 4A). Four out of all 8 MiSeq-positive FFPE samples were negative by qAS-PCR. Therefore, we excluded FFPE samples and analyzed data from 95 DNA samples that had been purified from PLP-fixed or frozen tissues.

When [mut]/([wt]+[mut]) values were compared with mutant variant allele frequencies determined by MiSeq, the rank correlation coefficient was 0.785 (Spearman's correlation $P<0.001$) (Figure 4B and C). Among the 95 samples analyzed, 38 (29 AITL and 9 PTCL-NOS) were judged positive and 57 (14 AITL and 43 PTCL-NOS) were judged negative by MiSeq. By comparison, when the cut-off level for [mut]/([wt]+[mut]) values was set at 1.5×10^{-2}, according to ROC curve (Supplemental Figure 1), 38 cases were judged positive for the G17V *RHOA* mutation, including 29 AITL and 9 PTCL-NOS. Overall, 91 of 95 specimens showed concordant results using both methods, while 4 cases showed discordant results (Figure 4B and C). If we assume that data generated by MiSeq is accurate, then the sensitivity and specificity of qAS-PCR were as high as 94.7% and 96.5%, respectively. Positive and negative concordance rates of the two methods were 94.7% and 96.5%, respectively (Table 4, Table S1 in File S1).

The four cases showing discordant results provided us with an insight into the comparison between MiSeq and aAS-PCR. Two samples were positive only based on MiSeq, and two were positive only by qAS-PCR. When we performed HISEQ2000 sequencing [12] for all these four samples, we observed $\geqq 0.02$ mutation allele frequencies in two samples. One had been deemed positive only by qAS-PCR and the other only by MiSeq. The other two samples showed <0.02 mutation allele frequencies by HISEQ2000. One of them was judged as negative only by qAS-PCR and the other only by MiSeq. Overall, accuracy with qAS-PCR and MiSeq was comparable.

Table 4. Correlation between qAS-PCR and MiSeq.

Method	Standard	Samples		N*[1]	RCC*[2]	Sensitivity	Specificity	PPV*[3]	NPV*[4]
qAS-PCR	MiSeq	AITL and PTCL-NOS	non- FFPE	all	0.785	94.7	96.5	94.7	96.5
				original	0.735	100.0	95.5	91.7	100.0
				WGA*[5]	0.822	87.5	100.0	100	86.7
			FFPE *[6]	13	0.919	87.5	80.0	87.5	80.0

*[1]N, number; *[2]RCC, rank correlation coefficient; *[3]PPV, positive predictive value; *[4]NPV, negative predictive value; *[5]WGA, whole-genome amplification. *[6]FFPE, formalin-fixed/paraffin-embedded.

doi:10.1371/journal.pone.0109714.t004

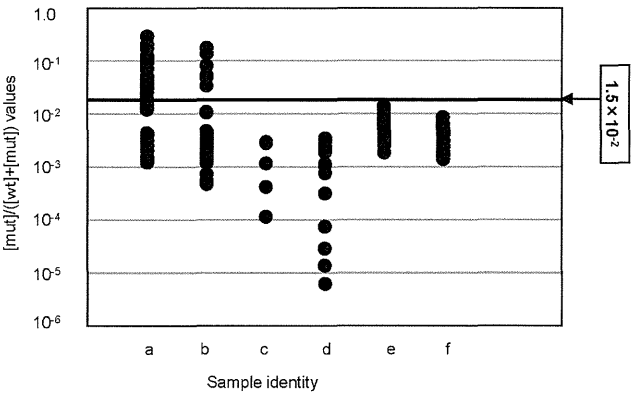

Figure 5. qAS-PCR for 275 tumor and control samples. qAS-PCR was performed for tumor samples, including 43 AITL (a), 52 PTCL-NOS (b), 5 T-cell lymphoma other than AITL and PTCL-NOS (c), 19 B-cell lymphomas (d), 129 myeloid malignancies (e) and 27 control samples (f).

doi:10.1371/journal.pone.0109714.g005

The qAS-PCR method using 50 ng of whole-genome-amplified DNA did not provide a robust correlation with the Miseq data for FFPE samples. The main reason was likely to be fragmentation of genomic DNA. To overcome this limitation, DNA prepared from the 13 FFPE samples was pre-amplified by PCR prior to performing qAS-PCR. Sensitivity and specificity for FFPE samples using amplicon was 87.5% and 80.0%, respectively, based on the mutation allele frequencies determined by MiSeq. (Figure 4D, Table S2 in File S1). Therefore, even for FFPE samples, the qAS-PCR method could robustly estimate the G17V RHOA mutation allele frequencies.

Effect of whole-genome amplification for qAS-PCR

When we divided the 95 samples into original DNA and whole-genome-amplified DNA cohort, sensitivity and specificity were 100% and 95.5% for original DNA cohort, and 87.5% and 100% for whole-genome-amplified DNA cohort, respectively (Supplemental Figure 2A-D, Table S3A and B in File S1).

In order to determine whether amplification influences the evaluation of mutation allele frequency by qAS-PCR, we compared the data for 15 pairs of original and whole-genome-amplified samples. Fourteen out of 15 pairs showed concordant results with each other (Table S3C and D in File S1, Figure S2E in File S1). One sample, which was judged positive by MiSeq, showed discordant results by qAS-PCR; positive for the original DNA and negative for the whole-genome-amplified DNA. As a summary, with some limitations, whole-genome-amplified DNA could provide robust results in most cases.

qAS-PCR for myeloid, B-cell and other T-cell malignancies

We performed qAS-PCR for buccal cells and non-tumor samples including bone marrow cells without lymphoma infiltration obtained from lymphoma patients, and confirmed that the qAS-PCR values were below the cut-off level in all samples. Then, we applied qAS-PCR for 153 tumor samples other than AITL and PTCL-NOS, including 129 myeloid, 19 B-cell, and 5 T-cell malignancies. Sanger sequencing also showed no mutant signals for any of these samples. All qAS-PCR values calculated using these samples were below the cut-off level (Figure 5).

Discussion

Our recent discovery of the highly frequent G17V *RHOA* mutation in AITL and AITL-like PTCL-NOS led us to develop a novel method to detect this mutation [12]. The results of qAS-PCR analysis described here are correlated well with those derived from deep sequencing (Table 4), while qAS-PCR is superior to deep sequencing in terms of the cost and convenience. There is a pressing clinical need for a well-validated *RHOA* testing method with optimal analytical performance using the least amount of difficult-to-obtain patient specimens. We show here that even DNA samples subjected to whole-genome amplification or low quality/concentration DNA extracted from FFPE samples can serve as reliable material for our qAS-PCR method, if appropriate PCR procedure and primers are used. Allele-specific PCR for G17V *RHOA* mutation was mentioned in other report [13], although sensitivity and specificity of the methods were not described.

In a previous study, we defined the cut-off level of mutant allele frequencies determined by MiSeq as 0.02 [12]. In this study, we defined the cut-off level as 1.5×10^{-2} for qAS-PCR, but it remains to be determined whether these cut-off levels are sufficient to detect AITL. Given our finding that the mutated *RHOA* allele frequencies distributed below 0.05 in many AITL samples [12], the tumor cell content might be very low and could be detected in some cases only when the cut-off levels of qAS-PCR and deep sequencing are lowered. If we set the cut-off value lower, the sensitivity should be improved with the increase of false-positive results, raising a dilemma common to other clinical testings.

Several hotspot mutations that reveal distinct hematologic malignancies have been identified in conditions other than T-cell lymphomas. For example, detection of the V617F *JAK2* mutation is a part of the diagnostic criteria for myeloproliferative neoplasms in the latest version of WHO classification [1], although consensus is not reached about the detection methods and cut-off levels. Methods have been developed to detect this mutation including allele-specific PCR and a PCR-restriction fragment length polymorphism (RFLP) approach utilizing mutation sequence specificity for a restriction enzyme[15–18]. More recently, a V600E *BRAF* mutation in hairy cell leukemia [19], an L265P *MYD* mutation in Waldenström macrogloblinemia [20], and several mutations in *STAT3* in large granular lymphocytic leukemia [21] have been identified as diagnostics of these tumor types. In the future, it is likely that molecular alterations, including the G17V *RHOA* mutation, will be increasingly incorporated into the diagnostic criteria for hematologic malignancies. In summary, our novel method to detect the G17V *RHOA* mutation could provide an important clinical tool to diagnose AITL and AITL-like PTCL-NOS and in the future serve as a means to classify AITL and PTCL-NOS.

Supporting Information

File S1 Figures S1–S2 and Tables S1–S4. Figure S1. ROC curve for data of qAS-PCR and MiSeq. Horizontal axis shows 1-specificity and Vertical axis shows sensitivity of qAS-PCR method compared to the data of MiSeq. Figure S2. Effect of whole-genome amplification for qAS-PCR A, Comparison of [mut]/([wt]+[mut]) values by qAS-PCR and mutant allele frequencies as determined by MiSeq for 66 original samples (linear). B, Comparison of [mut]/([wt]+[mut]) values by qAS-PCR and mutant allele frequencies as determined by MiSeq for 66 original samples (log scale). C, Comparison of [mut]/([wt]+[mut]) values by qAS-PCR and mutant allele frequencies as determined by MiSeq for 29 whole-genome amplified samples (linear). D, Comparison of [mut]/([wt]+[mut]) values by qAS-PCR and mutant allele frequencies as determined by MiSeq for 29 whole-genome amplified samples (log scale). E, Comparison of [mut]/([wt]+[mut]) values by qAS-PCR for 15 pairs of original and whole-genome amplified samples in a log scale.
(PDF)

Acknowledgments

We thank T Arinami for licensing the machine.

Author Contributions

Conceived and designed the experiments: RN-M MS-Y SC. Performed the experiments: RN-M. Analyzed the data: RN-M MS-Y KY SY Y. Shiozawa TN KS MS SO KT NN. Contributed reagents/materials/analysis tools: TE HM NO T. Kato NK YY KI YO SS T. Komeno Y. Sato TI IK. Contributed to the writing of the manuscript: RN-M MS-Y SC.

References

1. Swerdlow SH, Campo E, Harris NL, Jaffe ES, Pileri SA, et al. (2008) WHO classification of tumors of haematopoietic and lymphoid tissues. 4th ed. Lyon, France. IARC Press: 306–311.
2. de Leval L, Gisselbrecht C, Gaulard P (2010) Advances in the understanding and management of angioimmunoblastic T-cell lymphoma. Br J Haematol 148: 673–689.
3. Frizzera G, Moran EM, Rappaport H (1974) Angio-immunoblastic lymphadenopathy with dysproteinaemia. Lancet 1: 1070–1073.
4. Dogan A, Attygalle AD, Kyriakou C (2003) Angioimmunoblastic T-cell lymphoma. Br J Haematol 121: 681–691.
5. de Leval L, Rickman DS, Thielen C, Reynies A, Huang YL, et al. (2007) The gene expression profile of nodal peripheral T-cell lymphoma demonstrates a molecular link between angioimmunoblastic T-cell lymphoma (AITL) and follicular helper T (TFH) cells. Blood 109: 4952–4963.
6. Piccaluga PP, Fuligni F, De Leo A, Bertuzzi C, Rossi M, et al. (2013) Molecular profiling improves classification and prognostication of nodal peripheral T-cell lymphomas: results of a phase III diagnostic accuracy study. J Clin Oncol 31: 3019–3025.
7. Papadi B, Polski JM, Clarkson DR, Liu-Dumlao TO (2012) Atypical angioimmunoblastic T-cell lymphomas masquerading as systemic polyclonal B-immunoblastic proliferation. Virchows Arch 461: 323–331.
8. Couronne L, Bastard C, Bernard OA (2012) TET2 and DNMT3A mutations in human T-cell lymphoma. N Engl J Med 366: 95–96.
9. Cairns RA, Iqbal J, Lemonnier F, Kucuk C, de Leval L, et al. (2012) IDH2 mutations are frequent in angioimmunoblastic T-cell lymphoma. Blood 119: 1901–1903.
10. Delhommeau F, Dupont S, Della Valle V, James C, Trannoy S, et al. (2009) Mutation in TET2 in myeloid cancers. N Engl J Med 360: 2289–2301.
11. Langemeijer SM, Kuiper RP, Berends M, Knops R, Aslanyan MG, et al. (2009) Acquired mutations in TET2 are common in myelodysplastic syndromes. Nat Genet 41: 838–842.
12. Sakata-Yanagimoto M, Enami T, Yoshida K, Shiraishi Y, Ishii R, et al. (2014) Somatic RHOA mutation in angioimmunoblastic T cell lymphoma. Nat Genet 46: 171–175.
13. Palomero T, Couronne L, Khiabanian H, Kim MY, Ambesi-Impiombato A, et al. (2014) Recurrent mutations in epigenetic regulators, RHOA and FYN kinase in peripheral T cell lymphomas. Nat Genet 46: 166–170.
14. Wangkumhang P, Chaichoompu K, Ngamphiw C, Ruangrit U, Chanprasert J, et al. (2007) WASP: a Web-based Allele-Specific PCR assay designing tool for detecting SNPs and mutations. BMC Genomics 8: 275.
15. Zapparoli GV, Jorissen RN, Hewitt CA, McBean M, Westerman DA, et al. (2013) Quantitative threefold allele-specific PCR (QuanTAS-PCR) for highly sensitive JAK2 V617F mutant allele detection. BMC Cancer 13: 206.
16. Shammaa D, Bazarbachi A, Halas H, Greige L, Mahfouz R (2010) JAK2 V617F mutation detection: laboratory comparison of two kits using RFLP and qPCR. Genet Test Mol Biomarkers 14: 13–15.
17. Frantz C, Sekora DM, Henley DC, Huang CK, Pan Q, et al. (2007) Comparative evaluation of three JAK2V617F mutation detection methods. Am J Clin Pathol 128: 865–874.
18. Wu Z, Yuan H, Zhang X, Liu W, Xu J, et al. (2011) Development and inter-laboratory validation of unlabeled probe melting curve analysis for detection of JAK2 V617F mutation in polycythemia vera. PLoS One 6: e26534.

19. Tiacci E, Trifonov V, Schiavoni G, Holmes A, Kern W, et al. (2011) BRAF mutations in hairy-cell leukemia. N Engl J Med 364: 2305–2315.
20. Treon SP, Hunter ZR (2013) A new era for Waldenstrom macroglobulinemia: MYD88 L265P. Blood 121: 4434–4436.
21. Koskela HL, Eldfors S, Ellonen P, van Adrichem AJ, Kuusanmaki H, et al. (2012) Somatic STAT3 mutations in large granular lymphocytic leukemia. N Engl J Med 366: 1905–1913.

bjh research paper

Japan Clinical Oncology Group (JCOG) prognostic index and characterization of long-term survivors of aggressive adult T-cell leukaemia-lymphoma (JCOG0902A)

Takuya Fukushima,[1] Shogo Nomura,[2] Masanori Shimoyama,[3] Taro Shibata,[2] Yoshitaka Imaizumi,[4] Yoshiyuki Moriuchi,[5] Takeaki Tomoyose,[6] Kimiharu Uozumi,[7] Yukio Kobayashi,[8] Noriyasu Fukushima,[9] Atae Utsunomiya,[10] Mitsutoshi Tara,[11] Kisato Nosaka,[12] Michihiro Hidaka,[13] Naokuni Uike,[14] Shinichiro Yoshida,[15] Kazuo Tamura,[16] Kenji Ishitsuka,[16] Mitsutoshi Kurosawa,[17] Masanobu Nakata,[18] Haruhiko Fukuda,[2] Tomomitsu Hotta,[3] Kensei Tobinai[8] and Kunihiro Tsukasaki[19]

[1]Laboratory of Haematoimmunology, School of Health Sciences, Faculty of Medicine, University of the Ryukyus, Nishihara-cho, [2]JCOG Data Centre, Multi-institutional Clinical Trial Support Centre, National Cancer Centre, Tokyo, [3]Multicentre-institutional Clinical Trial Support Centre, National Cancer Centre, Tokyo, [4]Department of Haematology, Atomic Bomb Disease and Hibakusha Medicine Unit, Atomic Bomb Disease Institute, Nagasaki University, Nagasaki, [5]Department of Haematology, Sasebo City General Hospital, Sasebo, [6]Division of Endocrinology, Diabetes and Metabolism, Haematology, Rheumatology (Second Department of Internal Medicine), Graduate School of Medicine, University of the Ryukyus, Nishihara-cho, [7]Department of Haematology and Immunology, Kagoshima University Hospital, Kagoshima, [8]Department of Haematology, National Cancer Centre Hospital, Tokyo, [9]Division of Haematology, Respiratory Medicine and Oncology, Department of Internal Medicine, Faculty of Medicine, Saga University, Saga, [10]Department of Haematology, Imamura Bun-in Hospital, Kagoshima, [11]Department of Haematology, Kagoshima City Hospital, Kagoshima, [12]Department of Haematology, Kumamoto University of Medicine, Kumamoto, [13]Department of Internal Medicine, National Hospital Organization Kumamoto Medical Centre, Kumamoto, [14]Department of

Summary

This study evaluated the clinical features of 276 patients with aggressive adult T-cell leukaemia-lymphoma (ATL) in 3 Japan Clinical Oncology Group (JCOG) trials. We assessed the long-term survivors who survived >5 years and constructed a prognostic index (PI), named the JCOG-PI, based on covariates obtained by Cox regression analysis. The median survival time (MST) of the entire cohort was 11 months. In 37 patients who survived >5 years, no disease-related deaths in 10 patients with lymphoma-type were observed in contrast to the 10 ATL-related deaths in other types. In multivariate analysis of 193 patients, the JCOG-PI based on corrected calcium levels and performance status identified moderate and high risk groups with an MST of 14 and 8 months respectively (hazard ratio, 1·926). The JCOG-PI was reproducible in an external validation. Patients with lymphoma-type who survived >5 years might have been cured. The JCOG-PI is valuable for identifying patients with extremely poor prognosis and will be useful for the design of future trials combining new drugs or investigational treatment strategies.

Keywords: adult T-cell leukaemia-lymphoma, Japan Clinical Oncology Group trials, long-term survivors, prognostic index.

First published online 14 June 2014
doi:10.1111/bjh.12962

Haematology, National Hospital Organization Kyushu Cancer Centre, Fukuoka, [15]*Department of Haematology, National Hospital Organization Nagasaki Medical Centre, Omura,* [16]*Department of Medicine, Division of Medical Oncology, Haematology and Infectious Diseases, Fukuoka University, Fukuoka,* [17]*Department of Haematology, National Hospital Organization Hokkaido Cancer Centre, Sapporo,* [18]*Department of Haematology, Sapporo Hokuyu Hospital, Sapporo, and* [19]*Department of Haematology National Cancer Centre Hospital East, Kashiwa, Japan*

Received 14 January 2014; accepted for publication 10 April 2014
Correspondence: Takuya Fukushima, MD, Laboratory of Haematoimmunology, School of Health Sciences, Faculty of Medicine, University of the Ryukyus, 207 Uehara, Nishihara, Okinawa 903-0215, Japan.
E-mail: fukutaku@med.u-ryukyu.ac.jp

Adult T-cell leukaemia-lymphoma (ATL) is a distinct peripheral T-lymphocytic malignancy associated with human T-cell lymphotropic virus type I (HTLV-1) (Uchiyama *et al*, 1977; Poiesz *et al*, 1980; Hinuma *et al*, 1981; Miyoshi *et al*, 1981; Yoshida *et al*, 1982). Classification of clinical subtypes into acute, lymphoma, chronic and smouldering was proposed based on prognostic factors, clinical features and the natural history of the disease (Shimoyama, 1991). Patients with aggressive ATL (i.e., acute, lymphoma and unfavourable chronic types) have frequently been treated as a subtype of aggressive non-Hodgkin lymphoma (NHL), whereas those with indolent ATL (i.e., favourable chronic and smouldering types) have been managed as a subtype of chronic lymphoid leukaemia (Shimoyama, 1994; Tobinai & Watanabe, 2004). Aggressive ATL typically has a very poor prognosis compared with aggressive B-cell lymphomas, such as diffuse large B-cell lymphoma and peripheral T-cell lymphoma excluding ATL (The International Non-Hodgkin's Lymphoma Prognostic Factor Project's, 1993; Shimoyama, 1994; Gallamini *et al*, 2004; Watanabe *et al*, 2010). In the 1980's, patients with aggressive ATL were reported to have a median survival time (MST) of approximately 8 months, with a 2-year survival rate of <5% because of the multidrug-resistant phenotype of their malignant tumour cells, rapid proliferation of the tumour cells, a large tumour burden with multi-organ failure, hypercalcaemia, and/or frequent opportunistic infections (Lymphoma Study Group, 1991; Shimoyama, 1991, 1994; Tobinai & Watanabe, 2004).

The Japan Clinical Oncology Group (JCOG)-Lymphoma Study Group (LSG) has conducted consecutive clinical trials to improve the survival of patients with ATL. Earlier trials (JCOG7801, JCOG8101, and JCOG8701) revealed poor prognosis of ATL compared with other aggressive NHLs (Shimoyama *et al*, 1988; Tobinai *et al*, 1994). Furthermore, the disappointing results with conventional chemotherapies in the 1980s and the proposal for a subtype classification of ATL led us to conduct clinical trials with new agents that exclusively targeted aggressive ATL. The first phase II trial, JCOG9109 (1991–1993), evaluated combination chemotherapy with deoxycoformycin, an inhibitor of adenosine deaminase, which had been effective as a single agent against relapsed or refractory ATL (Tobinai *et al*, 1992). However, the results were disappointing with an MST of 7 months, similar to the findings of previous JCOG-LSG trials (Tsukasaki *et al*, 2003). The next phase II trial, JCOG9303 (1994–1996), evaluated the chemotherapy regimen VCAP-AMP-VECP (LSG15) against aggressive ATL. This dose-intensified multi-agent chemotherapy consisted of vincristine, cyclophosphamide, doxorubicin (DXR) and prednisone (PSL) for VCAP, DXR, ranimustine and PSL for AMP, and vindesine, etopside, carboplatin and PSL for VECP, supported by granulocyte colony-stimulating factor and intrathecal (IT) prophylaxis with methotrexate (MTX) and PSL. This phase II trial showed promising results, with complete remission (CR) and overall response rates of 36% and 81%, respectively, and an MST of 13 months at the expense of haematological and other toxicities (Yamada *et al*, 2001). Based on these results, we proceeded to the phase III trial JCOG9801 (1998–2003), which compared a modified VCAP-AMP-VECP regimen (shortened from 7 to 6 courses), to which cytarabine was added to the IT prophylaxis, *versus* CHOP (cyclophosphamide, DXR, vincristine and PSL)-14 supported by granulocyte

colony-stimulating factor and IT prophylaxis identical to the former regimen. The CR and 3-year overall survival (OS) were higher in the modified VCAP-AMP-VECP arm than in the CHOP-14 arm (40% vs. 25% and 24% vs. 13% respectively), suggesting that the former is a more effective regimen at the expense of greater toxicity for patients with newly diagnosed aggressive ATL (Tsukasaki *et al*, 2007).

Through these 3 JCOG trials for patients with aggressive ATL, the 5-year OS was improved, from 5% in the 1980's to 15% in the 1990s. To characterize the long-term survivors of aggressive ATL and to develop a new prognostic index (PI) for the disease, we performed a combined analysis (JCOG0902A) of all the patients enrolled in the 3 JCOG trials.

Methods

Study population

A total of 276 patients who were registered in the 3 JCOG trials described above were enrolled in this study (Yamada *et al*, 2001; Tsukasaki *et al*, 2003, 2007). Some patients did not receive anti-viral therapy using interferon-alpha and zidovudine because these drugs for ATL was not covered by the National Health Insurance in Japan. The eligibility criteria for the 3 JCOG trials were detailed in previous reports (Yamada *et al*, 2001; Tsukasaki *et al*, 2003, 2007). Briefly, patients were eligible to participate if they had aggressive ATL (i.e., acute, lymphoma, or unfavourable chronic type) with no prior chemotherapy, were aged 15–69 years and had preserved organ functions, no proven central nervous system (CNS) involvement and a performance status (PS) of 0–3 or 4 due to hypercalcaemia caused by ATL. The diagnosis of ATL was made based on seropositivity for HTLV-1 antibody and histologically and/or cytologically proven peripheral T-cell malignancy. Monoclonal integration of HTLV-1 provirus was analysed in 104 of 276 patients studied. Among these 104 patients, integration was detected in 100 patients and not detected in four patients.

The PI for the JCOG trials, which we refer to as the JCOG-PI, was constructed from the data of patients who participated in these trials (training set) and was then applied to an external validation set. The external validation set consisted of 136 patients who had not participated in prior JCOG studies but had received anthracycline-containing regimens as initial chemotherapy at three sites (Nagasaki University Hospital, Nagasaki Medical Centre, and Sasebo City General Hospital) under the remit of the JCOG-LSG. These patients were a subset of those from a previous retrospective study (Katsuya *et al*, 2012) and their OS and corrected calcium levels were reviewed.

Data and analysis sets

The endpoint of this study was OS, defined as the duration between registration to each JCOG trial and death from any cause or censored at the last follow up in living patients. For the validation data set, we substituted the date of treatment initiation for the date of registration.

Candidate covariates were sex, age, Eastern Cooperative Oncology Group (ECOG) PS, B symptoms, clinical stage, liver involvement, lactate dehydrogenase, blood urea nitrogen (BUN), corrected calcium levels, serum total protein, serum albumin, white blood cell count, total (normal and abnormal) lymphocyte count, neutrophil count and platelet count. We excluded the treatment regimen from the covariates because our aim was to create an index that could stratify the patients' prognosis and be applicable to future clinical trials evaluating various promising regimens. Cut-off values were determined clinically by dividing the continuous biological and laboratory test variables into no more than three categories. The data of 193 patients with a complete set of candidate covariates were used for the training set (Fig 1).

The protocol of this study was reviewed and approved by the JCOG Protocol Review Committee.

Statistical analysis

Patients who survived >5 years were categorized according to ATL subtype (acute, lymphoma or unfavourable chronic types). In addition, to evaluate the ATL-related death events for each subtype, a disease-specific mortality curve was estimated, for only those patients who survived >2 years, by means of a competing risks framework (Kalbfleisch & Prentice, 2002). The proportion of patients who survived >5 and >10 years was calculated to evaluate the association between long-term survival and CR (including CR unconfirmed) for initial treatment. The proportion of cases with

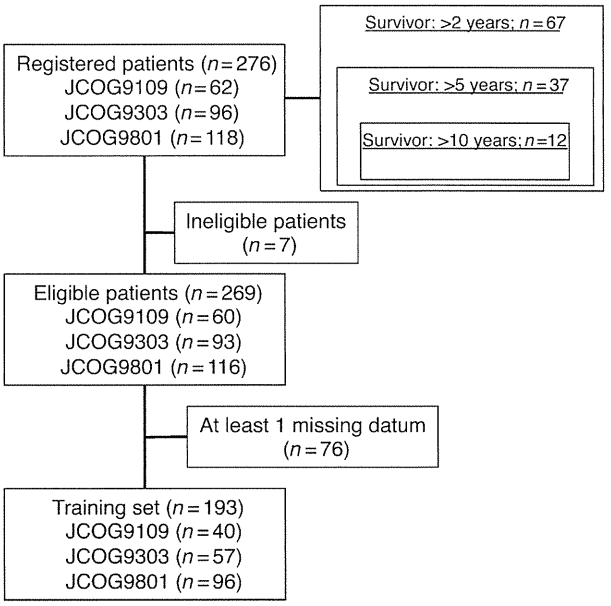

Fig 1. Patient disposition of the training set.

CNS involvement was compared among the JCOG trial regimens in an exploratory evaluation of the efficacy of prophylactic IT treatment. The prophylactic IT treatments against CNS involvement were: none in JCOG9109, MTX and PSL in JCOG9303, and MTX, cytarabine and PSL in both regimens in JCOG9801. Confidence intervals (CIs) for all the above proportions were computed using the Clopper–Pearson method (Clopper & Pearson, 1934).

Analyses for the development and validation of the JCOG-PI were performed according to a pre-specified analysis plan. The JCOG-PI consisted of risk groups that were developed using Cox's proportional hazards model. Before constructing the JCOG-PI, covariates with several definitions were selected for those with the smallest Akaike's Information Criteria (Akaike, 1973) on univariate analysis. Next, we verified the correlations between covariates to avoid multi-colinearity. Stepwise Cox regression analysis was then performed to identify unfavourable prognostic factors for constructing the JCOG-PI. The entry criterion was $P < 0{\cdot}20$ and the removal criterion was $P > 0{\cdot}15$.

The maximum number of risk group strata was set at three, based on the opinions of JCOG-LSG members who commented that too many strata were impractical for evaluating risk. The risk group was divided with patients equally distributed. The log-rank test was used to assess the discrepancy between the risk groups and the Kaplan–Meier method was applied to estimate OS.

All statistical analysis was performed using SAS Release 9·1 (SAS Institute, Inc, Cary, NC, USA). All reported P values are two-sided and $P < 0{\cdot}05$ was considered statistically significant.

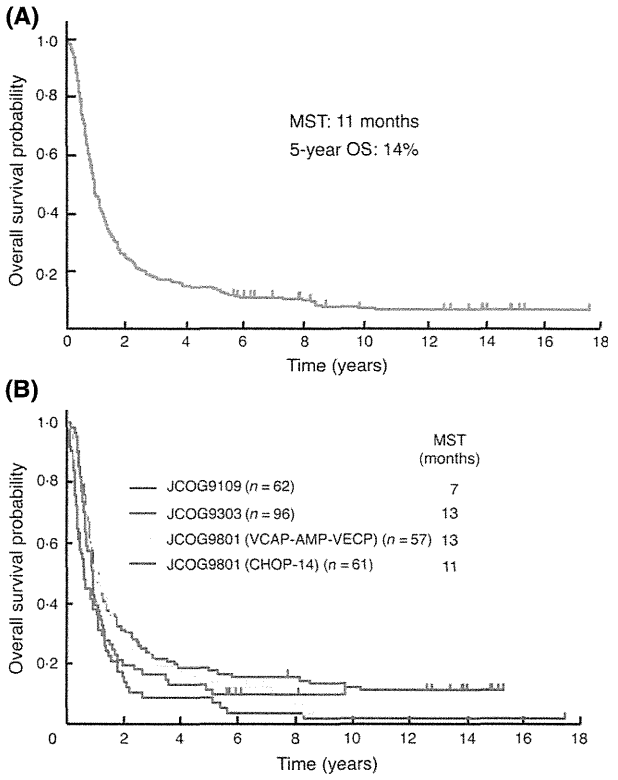

Fig 2. Overall survival (OS) of all registered patients in 3 Japan Clinical Oncology Group (JCOG) trials and according to treatment regimens. (A) OS of all 276 registered patients. Median survival time (MST) and the 5-year OS were 11 months and 14%, respectively.(B) OS according to different treatment regimens. MST was 7 months in JCOG9109, 13 months in JCOG9303, 13 months in VCAP-AMP-VECP of JCOG9801 and 11 months in CHOP-14 of JCOG9801.

Results

Patient characteristics

A total of 276 patients were registered in the 3 trials (JCOG9109, $n = 62$; JCOG9303, $n = 96$; and JCOG9801, $n = 118$) from 58 institutions in Japan. The MST and the 5-year OS of all patients were 11 months and 14% respectively (Fig 2A). The OS of each treatment regimen during the long follow up reconfirmed the findings of each original report (Fig 2B) (Yamada *et al*, 2001; Tsukasaki *et al*, 2003, 2007). Clinical characteristics are shown in Table I.

Long-term survivors according to subtype and initial response

The disease-specific mortality curve of patients who survived >2 years according to subtype is presented in Fig 3. Among the 37 patients (acute, $n = 22$; lymphoma, $n = 8$; unfavourable chronic, $n = 7$) who survived >5 years, there were no ATL-related deaths in lymphoma type, which was in contrast to the 10 ATL-related deaths in the acute and unfavourable chronic types after 5 years.

Of the 276 patients, 88 (32%) achieved CR with initial treatment. Of these 88 patients, 24 (27%) patients had survived >5 years and 11 (13%) patients had survived >10 years. Of the remaining 188 patients who did not achieve CR, 13 (17%) patients who survived >5 years and only 1 (0·5%) patient survived >10 years.

CNS involvement by treatment regimen

CNS involvement was 1·6% (95% CI, 0·04–8·7) in JCOG9109, 6·3% (95% CI, 2·3–13·1) in JCOG9303, and 3·5% (95% CI, 0·4–12·1) in the VCAP-AMP-VECP arm and 8·2% (95% CI, 2·7–18·1) in the CHOP-14 arm of JCOG9801. No significant differences in the proportion of CNS involvement were observed among the regimens.

Development of the PI

In univariate analyses, three covariates showed significant associations with OS, namely PS, corrected calcium level and serum total protein (all $P < 0{\cdot}05$; Table II). Stepwise Cox regression analysis returned three unfavourable prognostic